ABSTRACT

The project aims at the development of silicon doped tricalcium phosphate (Si-α-TCP) and at the preparation of the corresponding cements for bone tissue engineering applications.

There are two principal objectives into this project:

First, to optimize the parameters of a wet milling method in order to obtain Si-α-TCP with high purity.
Then, to use the Si-α-TCP produced as the main reactant to prepare calcium phosphate cements doped with silicon. The formation of Si-CDHA as final phase is evaluated.

The Si-α-TCP is prepared by milling hydroxyapatite and silicon oxide with water, followed by a heat treatment. In order to maximize the preparation of Si-α-TCP phase, some conditions have to be optimized: the reactants ratio, the milling process and the thermal treatment. The study carried out shows that a single stabilized α-TCP phase is produced when hydroxyapatite and silicon oxide, are milled according to a **0.48 SiO_2/HA molar ratio**, and heat treated at **1250°C during 2 hours**. The fact that silicon stabilizes the α-phase is revealed by the obtaining of this phase while no quench was performed.
A grinding process is carried out with the Si-α-TCP prepared to lead to the powder phase for cements. Finally, cement is prepared by mixing a calcium phosphate powder with water. The liquid to powder ratio is also adjusted in order to obtain cements with appropriate properties to be used for bone regeneration. Cement samples are stored under body simulated conditions and are evaluated at different time points.
The Si-α-TCP powder reacted with water with similar reaction kinetics than α-TCP powder free of silicon. Furthermore, cements prepared from Si-α-TCP powder have the same physic-chemical properties than cements prepared from α-TCP powder free of silicon. The studies performed were not conclusive on the silicon incorporation into the CDHA, and future studies will be required in order to evaluate this incorporation.

INDEX

ABSTRACT 1

INDEX 3

1. GLOSSARY 7

2. PREFACE 9

2.1. Origin of the project 9

2.2. Motivation 9

3. INTRODUCTION 11

4. THEORETICAL FUNDAMENTALS 13

4.1. Generalities on the hard tissues 13

4.1.1. Bone function 13

4.1.2. Bone types – hard tissues 13

4.1.3. Types of bone tissue 15

4.1.4. Bone composition 16

4.1.5. Bone remodeling 19

4.1.6. Fracture reparation 19

4.1.7. Non spontaneous bone reparation 21

4.2. Biomaterials 23

4.2.1. History of the biomaterials 24

4.2.2. Classification 24

4.2.3. Biomaterials for hard tissues applications 27

4.2.4. Tissue engineering 27

4.2.5. Calcium phosphates 28

4.2.6. Calcium phosphate cements 32

4.2.7. Advantages brought by silicon 36

4.2.8. Limits of calcium phosphate cements 38

5. STATE OF THE ART 39

6. MATERIAL AND METHODS ____ 41

6.1. General overview....41

6.2. The reactants....42

6.2.1. Characterization of the reactants....43

6.3. Preparation and characterization of Si-α-TCP....43

6.3.1. Theoretical fundamentals of milling....43

6.3.2. Preparation of Si-α-TCP....44

6.3.3. Heat treatment....47

6.3.4. Characterization of the Si-α-TCP....48

6.4. Preparation and characterization of cements....48

6.4.1. Grinding of the powder....48

6.4.2. Cements preparation....49

6.4.3. Characterization of the cements....50

7. CHARACTERIZATION TECHNIQUES ____ 51

7.1. X-Ray Diffraction....51

7.2. Inductively Coupled Plasma....53

7.3. Infrared spectroscopy....55

7.4. Scanning Electron Microscopy....56

7.5. Transmission Electron Microscopy....57

7.6. Laser granulometry....59

7.7. Nitrogen absorption....60

7.8. Helium pycnometer....61

7.9. Mercury Intrusion Porosimetry....62

7.10. Mechanical tests....63

8. RESULTS AND DISCUSSION ____ 65

8.1. Reactants....65

8.1.1. Phases and impurities present in the reactants....65

8.1.2. Particle size....68

8.2. Preparation and characterization of the powder 70
8.2.1. Influence of silicon – wet milling 70
8.2.2. Heat treatment Influence 75
8.3. Preparation and characterization of the Cements 79
8.3.1. Influence of grinding – particle size 79
8.3.2. Reaction kinetics 81
9. CONCLUSIONS ____ 93
10. RECOMMENDATIONS AND FUTURE PERSPECTIVES ____ 95
10.1 Recommendations 95
10.2 Future perspectives 95
11. ECONOMIC ASPECTS AND ENVIRONMENT IMPACT ____ 97
11.1 Economic aspects 97
11.1.1. Material 97
11.1.2. Characterization techniques 97
11.2. Environment impact 98
ACKNOWLEDGEMENTS ____ 99
BIBLIOGRAPHY ____ 101

1. GLOSSARY

α-TCP: α phase of the tricalcium phosphate, with chemical composition $Ca_3(PO_4)_2$.

β-TCP: β phase of the tricalcium phosphate, with chemical composition $Ca_3(PO_4)_2$.

Bioactivity: Characteristic of a material which has the ability to form a bond with living tissues. The bioactive materials have a better integration into the human body.

Biocompatibility: Said from those biomaterials which are accepted biologically into the body. The material accomplishes its specific function, giving place to a proper response of the receptor body in a concrete situation.

CaP: Calcium Phosphate

CDHA: Calcium deficient Hydroxyapatite. Said for those HA which have a Ca/P ratio lower than 1.67 In concrete, the CDHA is obtained from the dissolution and subsequent precipitation of tricalcium phosphate in aqueous solution, giving place to a chemical composition of $Ca_9(PO_4)_5(HPO_4)OH$.

CPC: Calcium Phosphate Cements

HA: Hydroxyapatite, with chemical composition $Ca_{10}(PO_4)_6(OH)_2$ corresponding to stoichiometric HA

Liquid to Powder Ratio (L/P): Ratio between liquid phase (mL) and powder phase (g) in which the calcium phosphate cements are prepared

Porosity: Percentage of empty volume in a material, part which is not occupied by solid fraction

Reabsorption: The act or process in which a material implanted into the body degrades chemically, being controllably absorbed, to finally be replaced for natural tissue.

Regeneration: A biomaterial that is progressively substituted by bone tissue newly formed until its complete extinction.

Ringer's Solution: Named after its inventor, the Ringer's solution is an aqueous solution with 0,9 wt % of NaCl that pretends be similar to the physiologic body fluids.

Setting reaction of cements: Initial transformation of a calcium phosphate cement formed for a powder phase and a liquid phase. The initial plasticity of the past is being lost due to

the precipitation of the most insoluble calcium phosphate in a form of entanglement crystals.

Si-α-TCP: α phase of the tricalcium phosphate doped with silicon

Si-CPC: Calcium Phosphate Cements doped with silicon

Glossary of techniques used

BET: The abbreviation corresponds to the first initial of the three discovers of the technique to measure the specific surface

ICP-MS: Inductively Coupled Plasma where the detector used is a Mass Spectroscopy

ICP-OES: Inductively Coupled Plasma where the detector used is an Optic Emission Spectroscopy

IR: Infrared spectroscopy

MIP: Mercury Intrusion Porosimetry

SEM: Scanning Electron Microscope

TEM: Transmission Electron Microscope

XRD: X Ray Diffraction

2. PREFACE

2.1. ORIGIN OF THE PROJECT

This Project takes place in the European curses of the EEIGM (European School of Materials Engineering). The objective is to make the students discover the research field and prepare them to work in this area. Laboratories belong to the Material Sciences and Metallurgy Department of one of the four partner universities.

2.2. MOTIVATION

There are two principal objectives into this project, the optimization of Si-α-TCP and the preparation of the corresponding silicon doped calcium phosphate cements:

The main interest of obtaining **Si-α-TCP** is:

▪ The stabilization of α-TCP by introducing silicon into its structure. This stabilization is due to alfagenic properties of this silicon, and may allow the temperature reduction of the thermal treatment. It might also avoid the usual quenching. It represents a significant advantage from a technical point of view, since the material could be cooled down slowly inside the furnace, avoiding the thermal shocks for the furnace components.

On the other hand, the main interest of the preparation of **silicon doped calcium phosphate cements** is:

▪ The potential enhancement of the cement bioactivity by the introduction of silicon into the cement end-product. Moreover, it is expected an improvement on the cell differentiation and differentiation. Nevertheless, this project does not pretend to evaluate such biologic properties, but to analyze some physic-chemical properties of the cements prepared.

3. INTRODUCTION

According to the United Nations (UN), demographic forecasts show that, in roughly 50 years' time, the percentage of over-60 years old in industrialized countries will have virtually doubled, from 20 to 35 percent of the overall population [1]. Therefore, the worldwide growing population longevity leads to an increase of bone diseases such as the osteoporosis, which causes the reduction of the bone mineral density (BMD).
Generally speaking, in bone diseases the bone microarchitecture is disrupted and the amount and variety of non-collagenous proteins in bone is altered. These changes on the bone morphology increase the risk of daily-life accidents, causing bone fracture.

Nowadays in orthopedic medicine, most bone defects are repaired using autografts, so-called "Gold Standard" due to their wide application. This bone graft is sourced from a patient's own bone in order to fill space, and produce an osteogenic response in the bone defect. However, the autograft has associated some problems: donor-site morbidity, lack of availability and need to operate twice the patient. Because of that, during the last decades has been increased the research on the biomaterials field. This is a promising area in constant evolution.

In the area of biomaterials, the calcium phosphates have been studied for bone repair applications over 80 years. Among the calcium phosphates, the α-TCP is widely used as a reactant of calcium phosphate cements. However, its preparation requires a high thermal treatment and so, a high level of energy. Moreover, although it has been studied that calcium phosphates are bioactive, this property can be improved.
The goal of this project is to prepare and characterize Si-α-TCP and bioactive calcium phosphate cements doped with silicon. The advantages that silicon brings are the stabilization of α-phase, enhancing at the same time the bioactivity of the cements prepared.
Nevertheless, an exhaustive characterization to evaluate whether the silicon has been incorporated into the lattice of the end product cement is out of this study.

4. THEORETICAL FUNDAMENTALS

4.1. GENERALITIES ON THE HARD TISSUES

4.1.1. BONE FUNCTION

Bones are rigid organs that form part of the endoskeleton of vertebrates. The most important function of bones is to provide a perfect framework to the body. They are also the responsible to synthesis blood cells. In the following table are listed the different functions that bones in the body and also are explained several examples for each one.

Function	Examples
Support	Bones of the legs, pelvis and vertebral column hold up the body; the mandible supports the teeth; nearly all bones provide support for muscles; many other soft organs are directly or indirectly supported by nearby bones.
Protection	Bones enclose and protect the brain, spinal cord, lungs, heart, pelvic viscera and bone marrow.
Movement	Skeletal muscles would serve no useful purpose if not for the rigid attachment and leverage provided by bones. Leg and arm movements are the most obvious examples; a less obvious one is that ventilation of the lungs depends on movement of the ribs by skeletal muscles.
Blood formation	Red bone marrow is the major producer of blood cells, including most cells of the immune system.
Electrolyte balance	The skeleton is the body's main mineral reservoir. It stores calcium and phosphate and releases them according to the body's physiological needs.
Acid-base balance	Bone buffer the blood again excessive pH changes by absorbing or releasing alkaline mineral salts.

Table 4.1: functions of the bones and its corresponding examples

4.1.2. BONE TYPES – HARD TISSUES

The skeletal system is one of the characteristics of mammals, since it is only present in this group (shells in mollusks are not bones). Every specie has the same structure bone structure, which can be separated into five different bone types [2]:

- **Long bones:** Bones connected with large movement. They are long and cylindrical with growth heads – epiphyses at either end. The epiphysis is covered by articular cartilage. Examples of long bones include the femur (thigh bone), the humerus (upper bone in the arm) and the phalanges (fingers and toes).
- **Short bones:** Almost cube shaped and associated with smaller and more complex movements such as the carpals (small bones in the base of the hand) and tarsals (in the feet).
- **Flat bones:** Protect the internal organs and include the skull (cranium), ribs, scapula (shoulder blade), sternum (breast bone) and the pelvic girdle.
- **Irregular bones:** Irregular in shape. Examples of this type include the vertebrae and some facial bones.
- **Sesamoid bones:** Small bones held within tendons that include a patella (knee cap). Cartilage separates the femur and the patella, and acts as a shock absorber.

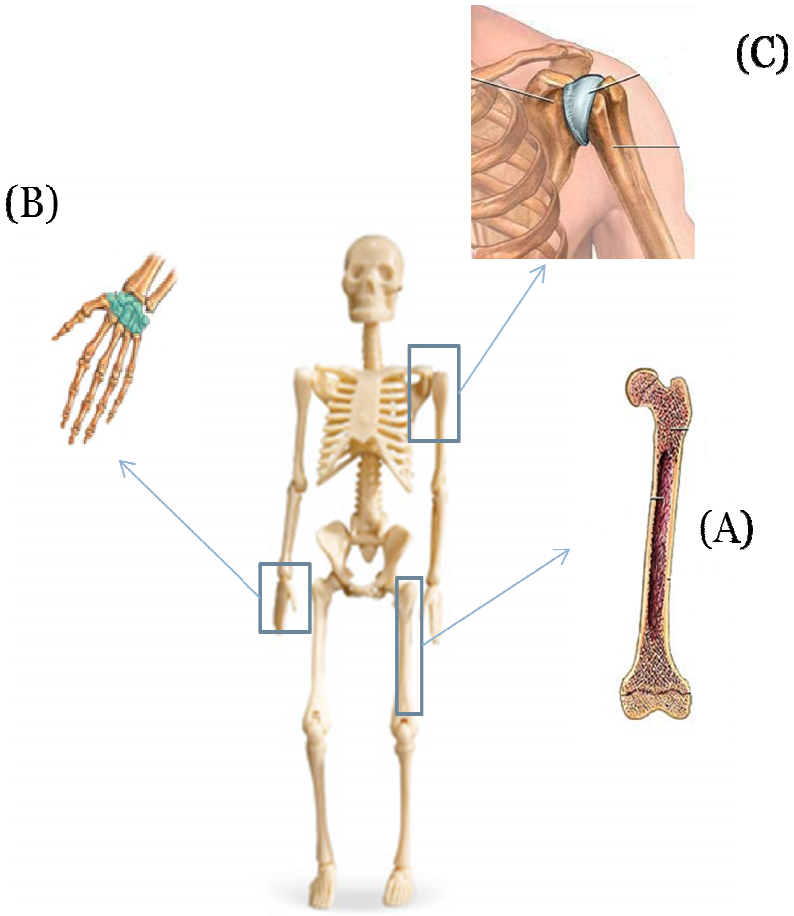

Fig 4.1: types of bones. Examples of bone type include (A) long bones (humerus), (B) flat bones (scrapula) and (C) short bones (metacarpal)

4.1.3. TYPES OF BONE TISSUE

Bone tissue is the main element of the skeletal system and has a specialized form of connective tissue. It is composed of cells and an extracellular matrix in which fibers are embedded. Its extracellular matrix, unlike other connective tissues, is calcified, conferring to it a high strength.

There are two types of bone tissue: the outer layer of the bone is dense and called "compact bone", whereas the inside part of the bone is spongy and named "cancellous bone".

- **Compact Bone**

The compact bone consists of closely packed osteons or haversian systems. The osteon is formed for a central canal, called the osteonic (haversian) canal, which is surrounded by concentric rings (lamellae) of matrix. Between the rings of matrix, the matured bone cells (osteocytes) are located in spaces called lacunae. Small channels (canaliculi) radiate from the lacunae to the haversian canal to provide passageways through the hard matrix. The haversian systems are packed tightly together to form what appears to be a solid and dense mass. The osteonic canals contain blood vessels that are parallel to the long axis of the bone. These blood vessels are interconnected, by way of perforating canals, with the surface of the bone.

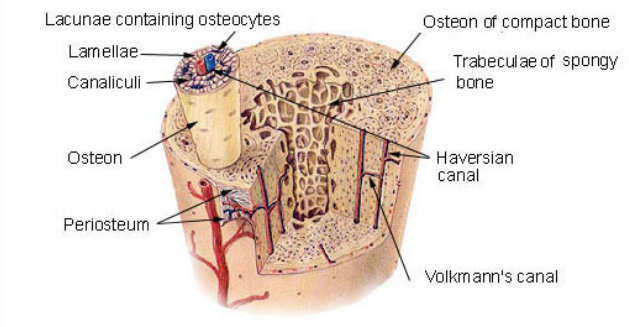

Figure 4.2: Representation of the compact and cancellous bone (from Arnold [3])

- **Cancellous Bone**

Cancellous bone is lighter and less dense than compact bone. This part of the bone consists on plates (trabeculae) and bars of bone adjacent to small, irregular cavities that contain red bone marrow. The canaliculi connect to the adjacent cavities, instead of a central haversian canal, to receive their blood supply. It may appear that the trabeculae

are arranged in a random manner, but they are organized to provide maximum strength similar to braces that are used to support a building. The trabeculae of spongy bone follow the lines of stress and can realign if the direction of stress changes.

In the following table are the mechanical properties of the bones (cortical and cancellous):

Properties	Cortical bone	Cancellous bone
Compression Resistance (MPa)	100 – 230	2 – 12
Torsion resistance (MPa)	50 – 150	–
Elastic modulus (GPa)	7 – 30	0.05 – 0.5

Table 4.2: Physical and mechanical properties of the cortical and cancellous bone [4]

4.1.4. BONE COMPOSITION

The composition of the bones is similar for all the different kinds. Next schema shows the composition of them:

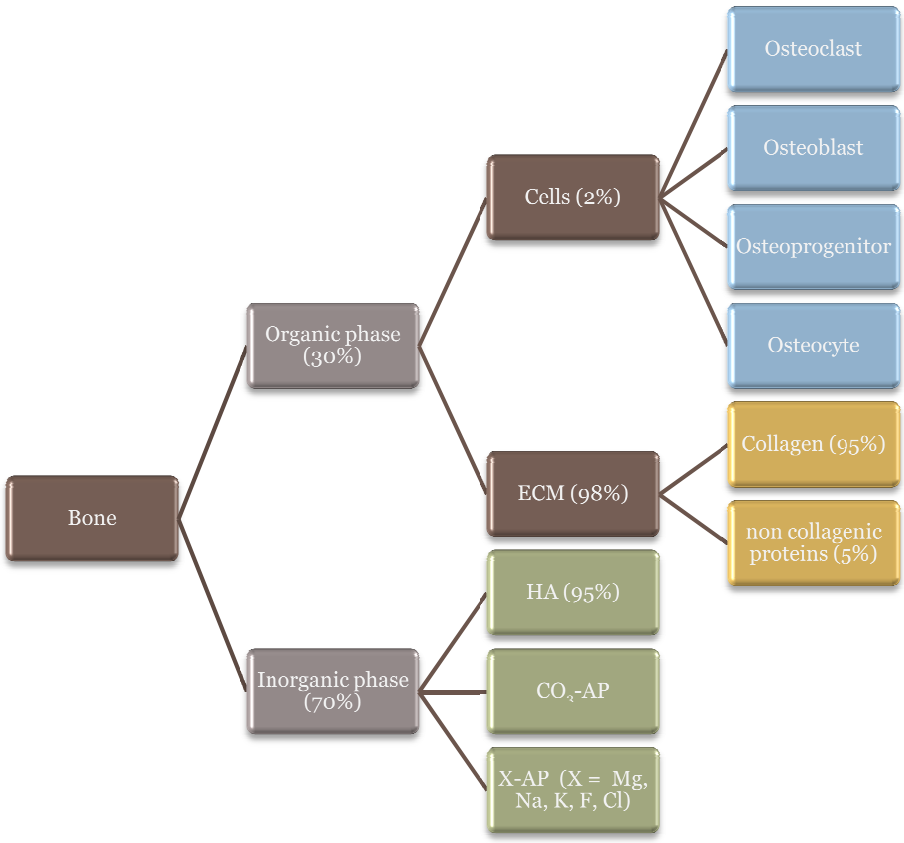

Fig. 4.3: Schema of the bone composition (adapted from Frank and Netter [5])

As shown, bone consists in a 30% of organic part and an inorganic one (70%). The organic is manly composed by an extracellular matrix (ECM) and bone cells (only a 2%, the rest being the ECM).

There are four types of cells which are constantly renewed in the bone: osteoblasts, osteocytes, osteoclasts and osteoprogenitors, and each of them have specific functions in order to cooperatively build up and constantly remodel the skeletal system. The osteoblasts are the cells encharged of bone formation and they also secrete mineral salts formed from calcium and phosphorus, which gives hardness to the bone..; osteoclasts resorb bone; osteocytes are mature osteoblasts; and osteoprogenitors are transformed osteocytes which carry out daily cellular activities. The equilibrium between osteoblasts and osteoclasts maintains bone tissue.

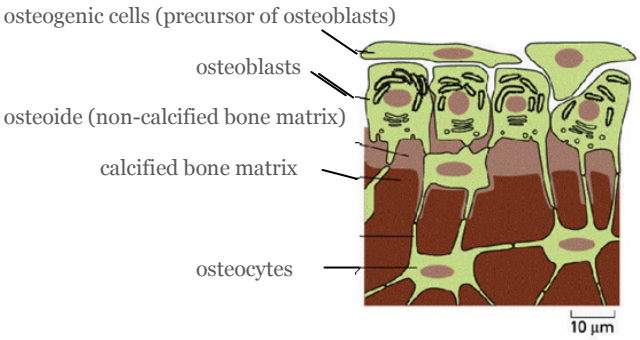

Fig. 4.4: Bone cells emplacement in the bone matrix [6]

The protein collagen (compose a 95% of the ECM) is the protein substance of the white fibers of the skin, bone, and connective tissues. It gives elasticity to bones so that they can give under the stresses generated by walking, lifting, and other activities. This protein is produced and secreted by osteoblasts. There are many other non-collagenic proteins in the ECM, such as osteocalcine, osteoreactant and proteglicans.

The inorganic part is mainly made of hydroxyapatite [7] (95% of this part). This natural HA is usually deficient of calcium, and because of that is more precise to call it calcium deficient hydroxyapatite (CDHA). The chemical nature of CDHA, which theoretical chemical formula is $Ca_9(HPO_4)(PO_4)_5(OH)$, lends itself to substitute its hydroxyl groups for elements or groups. Because of that, the rest of the inorganic phase is composed with substituted apatites. There are apatites with a high CO_3^{2-} concentration (CO_3-AP) and

apatites substituted with elements such as magnesium, sodium, potassium, fluor and chlorine.

Even though the mineral phase of the bone is mainly formed with calcium and phosphor, the bone can contain or at least interact with a series of metallic ions, which come from the blood fluid [8]. If those metallic ions interact with the bone, they can alter the specific functions of the osteoblasts and osteoclasts. In small fractions, bore and strontium, which have roles comportment in the metabolism close to calcium, can enhance the inhibition of osteoporosis. Also traces of silicon are also found in the bone. This element is fundamental for early stages of the bone metabolism, and it also enhances the cell proliferation during longlife.

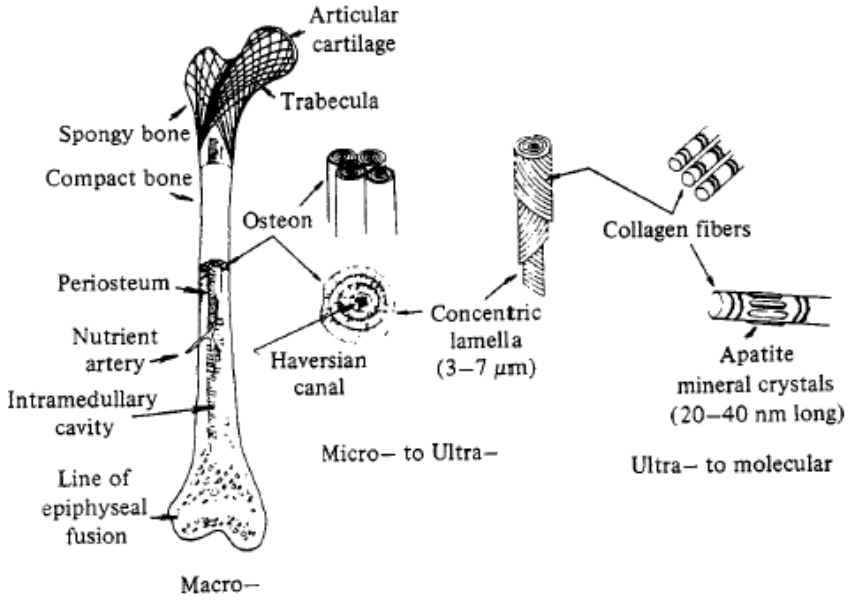

Fig 4.5: Hierarchical levels of structural organization in a human long bone [9]

Hydroxyapatite forms part of the crystallographic family of apatites, isomorphic compounds with the same hexagonal structure. HA molecules can group together (crystallize) to form microscopic clumps, called hydroxyapatite crystals.

Biologic HA presents a form of plates or needles of about 40–60 nm long, 20 nm wide, and 1.5–5 nm thick. They are deposited parallel to the collagen fibers, such that the larger dimension of crystals is along the long axis of the fiber.

4.1.5. BONE REMODELING

The skeletal system is characterized for its capacity to remodel itself in a complete manner, activating the embryogenesis processes. The embryogenesis is a continuous process of resorption and formation of hard tissue, in which the structure and morphology of the bones are modified until the characteristics of adult bonds are reached.

Bone remodelation cycle lasts for about 4 months. It starts with a **resorption phase**, during which some osteoclasts get differentiated and erode the osseous surface creating Howship's lacunas. After an apparent period of inactivity (the **inversion phase**) starts the **bone formation phase**. A group of osteoblasts get differentiated and refill the Howship's lacunas with new bone. This phase is also following for a period of inactivity, which is called **rest phase**. The following figure shows the process stages.

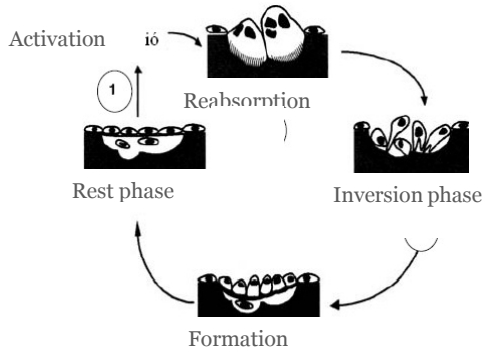

Fig 4.6: Schema of the stages of bone remodeling process [10]

4.1.6. FRACTURE REPARATION

Bones have the capacity to repair themselves with time when the breaking is not superior to the critical defect injury (see Fig 4.7). In the process of fracture healing, several phases of recovery facilitate the proliferation and protection of the areas surrounding fractures and dislocations.

The length of the process is relevant to the extent of the injury, and can depend upon the angle of dislocation or fracture. Usual margins between two to three weeks are given for the reparation of the majority part of upper bodily fractures.

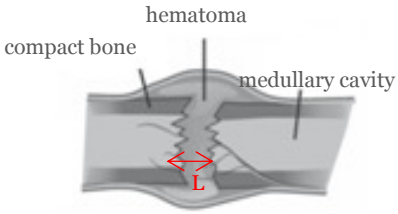

Fig. 4.7: Schema of a fracture. If the distance L between the two broken parts is superior to the critical defect injury L*, the bone repair itself with time

Even though a fracture ultimately heals through physiological processes, immobilization and surgery may facilitate it. In the radiograph below is shown a bone fracture in the process of healing.

Figure 4.8: X-Ray of a bone fracture in the process of healing with a bone graft

The healing process is mainly determined by the periosteum, the connective tissue membrane covering the bone. The periosteum is the primary source of precursor cells which develop into essential cells to the healing of bone: chondroblasts (a cell which originates from a mesenchymal stem cell and forms chondrocytes, commonly known as cartilage cells) and osteoblasts. The bone marrow (when present), endosteum, small blood vessels, and fibroblasts are secondary sources of precursor cells.

There are three major steps of fracture healing:

- Reactant Phase

After fracture, the first change is the presence of blood cells within the tissues which are adjacent to the injury site. Soon after fracture, the blood vessels constrict, stopping any further bleeding. Within a few hours after fracture, the extravascular blood cells, known as a "hematoma", form a blood clot. All of the cells within the blood clot, and some of those that are outside of the blood clot, but adjacent to the injury site, degenerate and die.

Within this same area, the fibroblasts survive and replicate. They form a loose aggregate of cells, interspersed with small blood vessels, known as granulation tissue.

- Reparative Phase

Days after fracture, the cells of the periosteum replicate and transform. The periosteal cells proximal to the fracture gap develop into chondroblasts and form hyaline cartilage. The periosteal cells distal to the fracture gap develop into osteoblasts and form woven bone. The fibroblasts within the granulation tissue also develop into chondroblasts and form hyaline cartilage. These two new tissues grow in size until they unite with their counterparts from other pieces of the fracture. This process forms the fracture callus. Rarely, if the callus formation is "hyperplastic" (or "exuberant"), there may be entrapment of adjacent tissues. Eventually, the fracture gap is bridged by the hyaline cartilage (a slimy mass of a firm consistency and with considerable elasticity which contains chondrocytes that produce the matrix) and woven bone, restoring some of its original strength.

The next step is the replacement of the hyaline cartilage and woven bone with lamellar bone. The lamellar bone begins forming soon after the collagen matrix of either tissue becomes mineralized. At this point, "vascular channels" with many accompanying osteoblasts penetrate the mineralized matrix. The osteoblasts form new lamellar bone upon the recently exposed surface of the mineralized matrix. This new lamellar bone is in the form of trabecular bone. Eventually, all of the woven bone and cartilage of the original fracture callus is replaced by trabecular bone, restoring most of the bone's original strength.

- Remodeling Phase

The remodeling process substitutes the trabecular bone with compact bone. The trabecular bone is first resorbed by osteoclasts, creating a shallow resorption pit known as a "Howship's lacuna". Then, osteoblasts deposit compact bone into this pit. Eventually, the fracture callus is remodeled into a new shape which closely duplicates the bone's original shape and strength.

4.1.7. NON SPONTANEOUS BONE REPARATION

There are two ways to repair a broken bone:

- **Substitution**: Implantation of an inert material (a prosthesis) into the damaged bone in order to just recover the function which has been lost.

- **Regeneration**: Introduction of a natural or synthetic material which enhances the regeneration of natural bone.

In the case of regeneration, bone grafting is commonly used to repair bone fractures that are very complex. A bone graft may be used when the fracture pose a significant risk to the patient, or when heal process fails.

The material introduced can be a healthy bone or a replacement material with the property to enhance the bone regeneration. When the selected material is placed into spaces between or around broken bone (fractures) or holes in bone (defects), speeds the healing process. Bone graft can be used to help fusion between vertebrae, correct deformities, or provide structural support for fractures of the spine. In addition to fracture repair, bone graft is also used to repair defects in bone caused by birth defects, traumatic injury, or surgery for bone cancer.

There are three ways in which a bone graft can help repair a defect. The first is called **osteogenesis**, the formation of new bone by the cells contained within the graft. The second is **osteoinduction**, a chemical process in which molecules contained within the graft (bone morphogenetic proteins) convert the patient's cells into cells that are capable of forming bone. The third is **osteoconduction**, a physical effect by which the matrix of the graft forms a scaffold on which cells in the recipient are able to form new bone.

New bone for grafting can have different sources and receives a different name on function of this. When is obtained from other bones in the patient's own body (e.g. hip bones or ribs) is called **autograft**; if it is taken from died people that is frozen and stored in tissue banks is named **allograft**. Finally, when the bone comes from other species is called **xenografts**.

A variety of natural and synthetic replacement materials are also used instead of bone, including collagen; polymers such as silicone and some acrylics; ceramics such as hydroxyapatite and calcium sulfate. Resorbable polymeric grafts are also being studied. These resorbable grafts provide a structure for new bone to grow on and, afterwards, the grafts are dissolved leaving the new bone behind.

Although the grafts are useful in many situations, they also present some problems. The drawbacks of autografts include:

- Additional surgery, including anesthesia to harvest, the bone for grafting;
- Added costs of the additional surgery;
- Pain and infection that might occur at the site from which the graft is taken; and

- Relatively small amount of bone that is available for grafting

Allografts also include some drawbacks:

- Variability between lots, since the bone is harvested from a variety of donors;
- Bone may take longer to incorporate with the host bone than an autograft would;
- Graft may be less effective than an autograft;
- Possibility of transferring diseases to the patient; and
- Complications may result from the immune response mounted by the patient's immune system against the grafted bone tissue. The immune rejection can be decreased when using anti-rejection agents

Finally, the xenografts show some problems similar to those explained before: the bone incorporation is less effective than in the case of autograft. Moreover, the transferring diseases and complications have also to be considerated.

The inconvenient presented for grafts lead to another solution to bone regeneration: the use of artificial materials that can be introduced and integrated into the body. This kind of materials are knows as **biomaterials**.

4.2. BIOMATERIALS

A biomaterial by definition is “a non-drug substance suitable for inclusion in systems which augment or replace the function of bodily tissues or organs” [11]. Nowadays, although the gold standard keeps being the autograft, the biomaterials are gaining more importance. Biomaterials have a high similarity to the natural tissues which have to regenerate, being incorporated into the body without exhibiting any of the drawbacks exposed on the hollow in the bone section.

The main property required of a biomaterial is that it does not illicit an adverse reaction when placed into service. These materials must also be capable of being in contact with bodily fluids and tissues for prolonged periods of time, whilst eliciting little if any adverse reactions. Biomaterials play an important role when it is stuck to the bone, which means that the bone needs to be helped in order to regenerate faster.

The range of applications is vast and includes artifacts such as joint and limb replacements, artificial arteries and skin, contact lenses, and dentures. While the implementation of some of these materials may be for medical reasons, such as the

replacement of diseased tissues required to extend life expectancies, other reasons may include purely esthetic ones, including breast implants. This increasing demand arises from an ageing population with higher quality of life expectations. The biomaterials community is producing and improving implant materials and techniques to meet the existing demand. The increasing demand of young patients also requires the mentioned improvement due to the necessity of enhanced properties [12].

4.2.1. History of the biomaterials

Some of the earliest biomaterial applications were as far back as ancient Phoenicia where loose teeth were bound together with gold wires for tying artificial ones to neighboring teeth. In the early 1900's bone plates were successfully implemented to stabilize bone fractures and to accelerate their healing. In the 1950's, blood vessel replacement were in clinical trials and artificial heart valves and hip joints were in development. It is already been a century that artificial materials and devices have been developed to a point where they can replace various components of the human body.

4.2.2. Classification

When a synthetic material is placed within the human body, tissue reacts towards the implant in a variety of ways depending on the material type. The mechanism of tissue interaction (if any) depends on the tissue response towards the implant surface. In general, there are three terms in which a biomaterial may be described in or classified into representing the tissues responses. These are bioinert, bioresorbable, and bioactive.

- The term **bioinert** refers to any material that once placed in the human body has a minimal interaction with its surrounding tissue and has an extremely slow kinetics of reaction. Generally, a fibrous capsule is formed around the implant due to the body intention to protect itself from an unknown body. Examples of bioinert materials are stainless steel, titanium, alumina, partially stabilized zirconium and high molecular weight polyethylene.
- **Bioactive** refers to a material, which upon being placed within the human body interacts with the surrounding bone and, in some cases, even with the soft tissue [13]. The bioactivity of a material is increased when an exchange reaction between the bioactive implant and the body fluids surrounding is produced. This reactions

result in the formation of a biologically active carbonate apatite (CO_3-Ap) layer on the surface of the implant that is chemically and crystallographically equivalent to the mineral phase of the bone. Consequently, bioactive materials encourage bonding to surrounding tissues, stimulating, for example, new bone growth. Prime examples of these materials are synthetic hydroxyapatite [$Ca_{10}(PO_4)_6(OH)_2$], glass ceramic A-W and bioglass®

- **Bioresorbable** is a material that upon placement within the human body starts to being resorbed at the same time that is slowly replaced by the advancing tissue (such as bone). This resorption is usually due to two complementary processes. On one hand, the material is dissolved for its intrinsic product of solubility. On the other hand, it is also resorbed by osteoclasts when remodeling processes are produced. Common examples of bioresorbable materials are tricalcium phosphate [$Ca_3(PO_4)_2$] and polylactic–polyglycolic acid copolymers. Calcium oxide, calcium carbonate and gypsum are other common materials that have been utilized during the last three decades.

Another classification that is widely used nowadays associate the terms which have been just explained in generations, being the third one the kind of materials which have a higher demand at present:

- The **first generation** concerns the bioinert materials such as Al_2O_3, ZrO_2, TiO_2.
- The **second generation** consists in the ceramics which are either bioactive OR bioresorbable. Examples of these are the synthesized hydroxiapatite, the bioactive glasses and the bioactive ceramics.
- Finally, the **third generation** of ceramics in tissues applications are the bioactive AND bioresorbable ones: α-TCP, β-TCP and DCPD (dicalcium phosphate dehydrate).
-

The following figure shows this classification inside a same application: a dental implant.

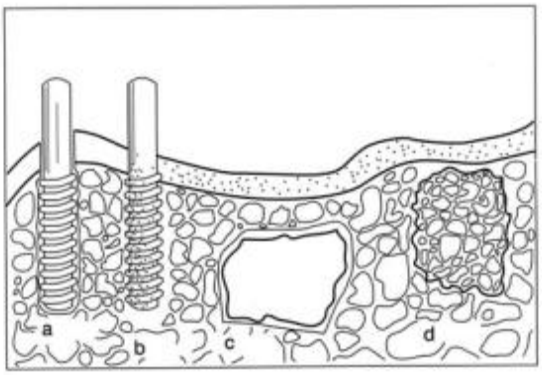

Figure 4.9: Classification of biomaterials according to their bioactivity: (a) bioinert alumina dental implant, (b) bioactive hydroxyapatite coating on a metallic dental implant, (c) surface active bioglass, and (d) bioresorbable tricalcium phosphate ($[Ca_3(PO_4)_2]$ implant (from Hennes *[14])*

The range of applications for biomaterials is large. The number of different biomaterials is also significant. Metallic, ceramic and polymeric biomaterials are used in orthopedic applications. However, in general:

- **Metallic biomaterials** are used for load bearing applications and must have sufficient fatigue strength to endure the rigors of daily activity eg walking, chewing etc. Metallic materials are normally used for load bearing members, such as pins and plates and femoral stems.
- **Ceramic biomaterials** are generally used for their hardness and wear resistance for applications such as articulating surfaces in joints and teeth, as well as bone bonding surfaces in implants. Ceramics such as alumina and zirconium are used for wear applications in joint replacements, while hydroxyapatite is used for bone bonding applications to assist implant integration.
- **Polymeric materials** are usually used for their flexibility and stability, but have also been used for low friction articulating surfaces. Polymers such as ultra high molecular weight polyethylene are used as articulating surfaces against ceramic components in joint replacements.

Some examples of biomaterials are provided in table 4.3

Metals	Ceramics	Polymers
316L stainless steel	Alumina	Ultra high molecular weight polyethylene
Co-Cr Alloys	Zirconia	Polyurethane
Titanium	Carbon	
Ti6Al4V	Hydroxyapatite	

Table 4.3: Some accepted biomaterials

A wide range of biomaterials are **composites**. It means that they are composed by more than one rage of materials, in order to enhance the desired properties

4.2.3. BIOMATERIALS FOR HARD TISSUES APPLICATIONS

The ultimate objective for the biomaterials research area is to create an artificial bone which would be equivalent to the natural one.

However, the biomaterials are already used in the hard tissues area: among them we can mention the Poly(HEMA), a collagen composite used as a biomaterial for hard tissue replacement [15]. There is also a study (Vago et al [16]) in which biofabricated coralline is used to replace the tissues. The research group in charge of the study incorporated a biofabricated matrix into a biphasic osteochondral area, and they observed that after 4 months the biomaterial had been completely replaced by new tissue).

4.2.4. TISSUE ENGINEERING

The bone tissue engineering is a biomedical emerging interdisciplinary field that seeks to address the needs on the biomaterials field by applying the principles of biology and engineering. The goal is to develop viable substitutes that restore and maintain the function of human bone tissues. This form of therapy differs from permanent implants in

that the engineered bone becomes integrated within the patient, affording a potentially permanent and specific cure of the disease state.

There are many approaches to bone tissue engineering, but all involve one or more of the following key ingredients: harvested cells, recombinant signaling molecules, and three-dimensional (3D) matrices. One popular approach involves seeding with cells and signaling molecules (e.g. protein growth factors) a highly porous biodegradable matrices (scaffolds), in the shape of the desired bone... Next step is culturing and implanting the scaffolds into the defect to induce and direct the growth of new bone. Inside the body, cells attached into the scaffold multiply and differentiate (i.e., transform from a nonspecific or primitive state into cells exhibiting the bone-specific functions). Finally, a healthy bone grows at the same time that the scaffold degrades.

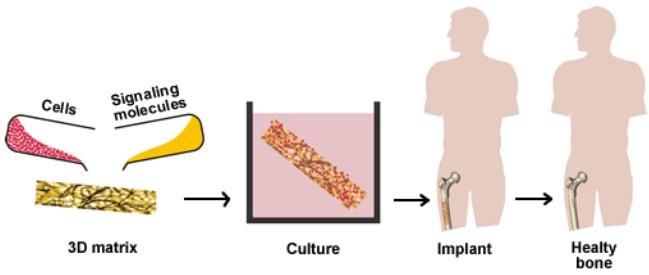

Figure 4.10: Scaffold-guided tissue regeneration

Nowadays, an important challenge in the tissue engineering field seems to be how to insure angiogenesis into the scaffold. The supply of blood is very important to maintain cells alive and enhance the regeneration process. Researchers are also focused on new biomaterials which cause minimal foreign body response and other that degrade in a completely predictable fashion. Also advanced manufacturing systems are required to fabricate complex scaffolds with spatially controlled distributions of materials, microstructures, cells and growth factors.

The tissue engineering is still a big challenge, although some surgeries have already successfully realized. In the case of applying this interdisciplinary field in the area of hard tissues, the scaffold could be prepared using ceramic materials as calcium phosphates.

4.2.5. CALCIUM PHOSPHATES

The calcium phosphates (CaPs) have been studied as potential materials for bone repair in the last 90 years. Albee was the first known researcher on this field. In 1920, he introduced a tricalcium phosphate (TCP) into an animal to study its efficiency as bone

substitute[17]. A significant progress of this material for medical application occurs between 1970 and 1980, when was discovered that bioglass (calcium phosphate glass) has osteoconductive properties [18-19]. Nowadays, the osteoconductives properties of CaP are recognized and they are widely used to produce biomaterials for osseous reparation.

The CaP introduced into the body can be eliminated in two different ways: either passively (dissolution due to its intrinsic product of solubility) and/or actively (the osteoclasts decrease the pH surrounding of the material, increasing the solubility). The most convenient is that the material disappears following the active way, because it is slower and more alike to the natural process.

For example, the CDHA is bioreabsorbible, and it goes away from the body for both active and passive mode.

In the following table are listed several well-known calcium phosphates with their main properties:

Compound	Chemical formula	Ca/P ionic ratio	Solubility at 25°C (10^{-Ks})
Monocalcium phosphate monohydrate	$Ca(H_2PO_4)_2{\cdot}H_2O$	0,5	1,14
Monocalcium phosphate anhydrous	$Ca(H_2PO_4)_2$	0,5	1,14
Dicalcium phosphate dehydrate, mineral brushite	$CaHPO_4{\cdot}2H_2O$	1	6,59
Dicalcium phosphate anhydrous, mineral monetite	$CaHPO_4$	1	6,90
Octacaclcium phosphate	$Ca_8(HPO_4)_2(PO_4)_5{\cdot}H_2O$	1,33	96,6
α-TCP	$\alpha\text{-}Ca_3(PO_4)_2$	1,5	25,5
β -TCP	$\beta\text{-}Ca_3(PO_4)_2$	1,5	28,9
CDHA	$Ca_{10-x}(HPO4)_x(PO4)_{6-x}(OH)_{2-x}$	1,5-1,67	~85,1
HA	$Ca_{10}(PO_4)_6(OH)_2$	1,67	116,8

Table 4.4: Main existing calcium phosphates obtained through thermal reactions or precipitation reactions, with their name, formulation, relation Ca/P (number of ca atoms per number of p atoms in the component) and their solubility (adapted from Dorozkhin [20])

The solubility in water is one of the most important properties of CaP, since the in vivo behavior of CaPs can be predicted in a large extent by their solubility [21]. If the solubility of a CaP is lower than the mineral part of the bone one, it will degrade extremely slowly [22]. In the previous table is showed the solubility of stoichiometric HA, which has a Ks = $10^{-116.8}$, is the lowest of the components presented. Thus, HA would be expected to have a long life time in the bones. Nevertheless, bones are mainly constituted for CDHA or substituted HA, what confers to it a higher solubility.

The most employed CaP as biomaterials are the hydroxyapatite (HA), the tricalcium phosphate (TCP) and the mix of this two, biphasic calcium phosphate (BCP). The difference between them is the intrinsic solubility and so the bioreabsorbation velocity.

The HA is the most used CaP in the implant fabrication area, since it is the most similar component to the mineral composition of the bones. Moreover it has advantageous properties, because is biocompatible, osteoconductible, bioactive, and possesses a good mechanical resistance, which is needed to alike to the mechanical bones properties.

The following diagram shows the changes of phases for the CaP.

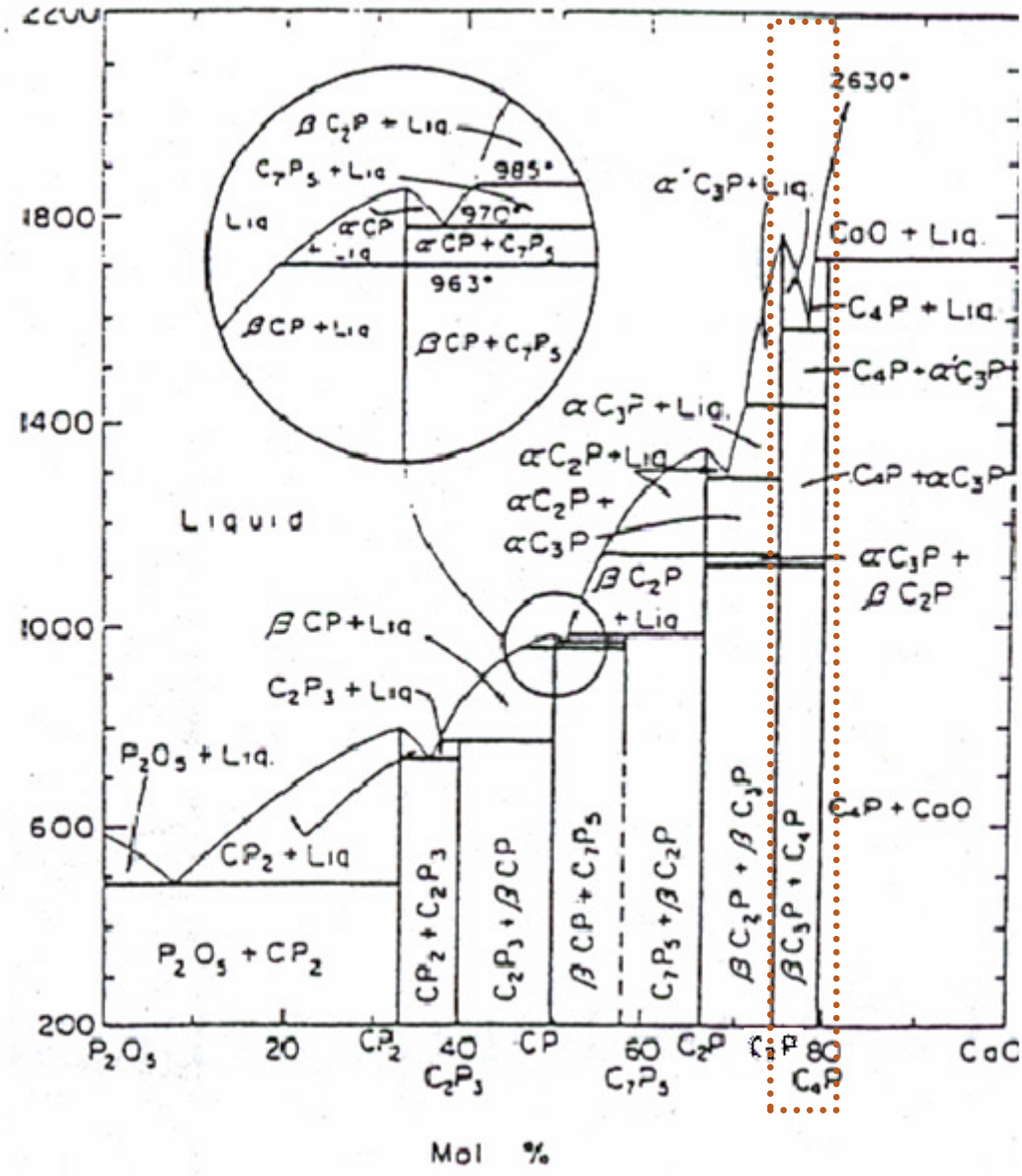

Figure 4.11: phase diagram of the system P_2O_5-CaO, representing the different components quantity, as a function of the molar percentage of CaO (from Barnes et al[23])

Due to the high complexity of the diagram phase exposed, next paragraphs are focused on the TCP which has a Ca/P ratio of 1.5 and is found in the Ca_3P area.

Observing the diagram phase from the bottom to the top, TCP phases are distinguished: β-TCP, α-TCP and α'-TCP.

To obtain each of these phases, a mixture of reactants with an adequate Ca/P ratio has to be prepared. A thermal treatment is necessary in order to produce a solid reaction. The β-phase is formed when the temperature applied is below 1180°C. As this is the stable phase at room temperature, any thermal treatment which is not followed by a quench gives this phase. The α-phase is obtained only if a temperature between 1180°C and 1400°C is reached and a quench is performed afterwards. Finally, the α'-phase is obtained if the temperature is raised over 1400°C and a quench is realized.

It is important to consider that the high-temperature α-phase is metastable at RT. Thus, it is possible to find β-TCP residues after the heat treatment due to a slow quench, or as a response of betagens impurities (e.g. Mg [59]) that stabilize the β phase.

Eventhough, β-TCP has the same chemical composition than α-TCP, they have different crystallographic structure. The higher solubility of α-TCP in front of β-TCP makes them convenient for different applications. While α-TCP produces an apatite product when in contact with water, being used as cement, β-TCP is used in different forms like granules or blocks.

Usually, in order to prepare an α-TCP, a mixture of $CaCO_3$ and $CaHPO_4$ is realized, keeping a Ca/P ratio of 1.5. Afterwards, a solid reaction is performed by calcining the material at 1300°C for several hours, followed by a quench [24].

4.2.6. CALCIUM PHOSPHATE CEMENTS

In the 1980s, a new biomaterial was introduced by Brown y Chow [25]: calcium phosphate cement. The first commercial CPC product was introduced about ten years ago for the treatment of maxilla-facial defects and deformities [26], as well as for the treatment of fracture defect [27]. Nowadays, the interest for these materials is still rising. Indeed, this type of material offers a large range of possibilities.

The CPC consists on a mixture of an aqueous solution and one or several powdery CaP. The mixture produces a moldable paste which hardens with time. It has also the big advantage of an acceptable clinical time, which means that the duration between the moment of injection of the paste and the hardening of the cement is coherent for a surgery application [28].

Consequently, calcium phosphate cements for bone regeneration are an important step in medical science, like for orthopedic surgery, dentistry, maxillofacial surgery and reconstructive surgery. To reach this promising goal, there are some important conditions

such as biocompatibility, controlled degradation, osteoconductivity, and formability.

Three main different kinds of cements can be differentiated: apatite (PHA), brushite (DCPC), and amorphous calcium phosphate (ACP). Apatite CPCs are usually prepared using α-TCP as reactant. This is due to the high solubility of the component, which transforms itself fast into CDHA. Apatite CPC are viscous and easily moldable, but tend to be difficult to inject. Nevertheless, their biocompatibility is normally excellent. Brushite CPC is slightly weaker than apatite CPC but degrades faster.

4.2.6.1. Preparation of CPCs

Generally speaking, the calcium phosphate bone cements consist on a mixture between one or various calcium phosphate powders with water or an aqueous solution (which contains an acid like H_3PO_4 or a salt such as Na_2HPO_4). The CaP gets dissolved in the aqueous solution and during setting CDHA precipitates (even at 37ºC) giving place to a solid body with high micro and nano porosity.

To understand why this process occurs in the way just described, next graph shows the solubility isotherms of several CaPs in water.

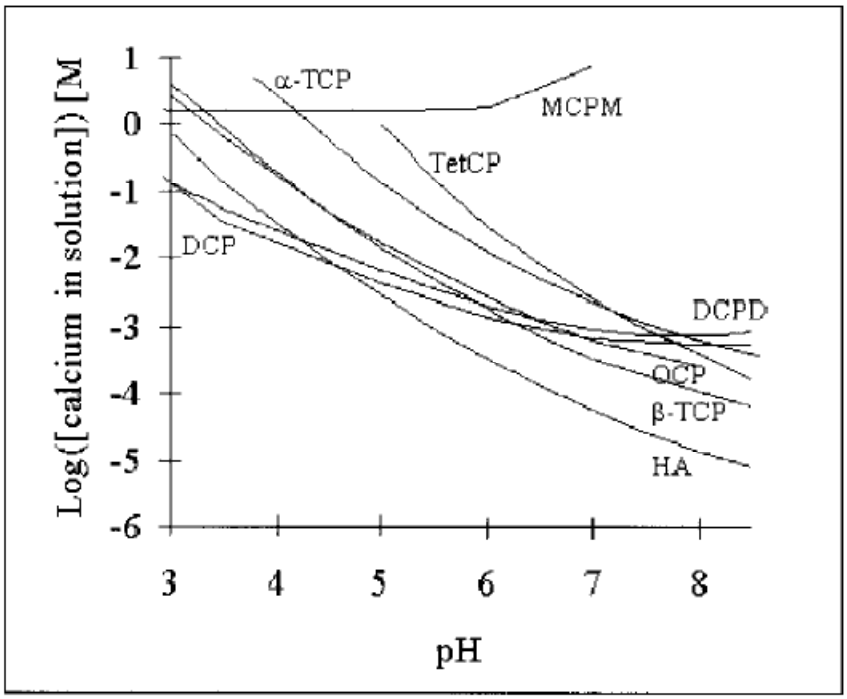

Figure 4.12: solubility isotherms of several CaPs in water. The solubility is expressed in the total amount of calcium ions in solution (From Vereecke and Lemaître [29])

The α-TCP is one of the most widely used CaP to prepare apatitic cements, due to its high solubility at physiological pH and room temperature. In water, this component dissolves fast giving place to the precipitation of the most insoluble CaP, hydroxyapatite. This CaP keeps the same Ca/P ratio as the reactant (Ca/P = 1.5) and this way is CDHA. In other words, this system is based on the hydrolysis of α-TCP to CDHA according to the following equation:

$$3\ \alpha\text{-}Ca_3(PO_4)_2 + H_2O \rightarrow Ca_9(HPO_4)(PO_4)_5(OH)\ [30]$$

When apatitic cements are prepared, α-TCP is the main reactant due to its higher solubility. Because of that, this component dissolves fast giving place to the precipitation of the most insoluble CaP, the HA (which keeps the same Ca/P ratio as the reactant, being so CDHA). This precipitation reaction and the following growth and entanglement of the CDHA crystals, is the reason for the progressive hardenening of the paste, finally providing a mechanical rigidity and converting it into a solid body.

Here is the overall method to prepare CPCs:

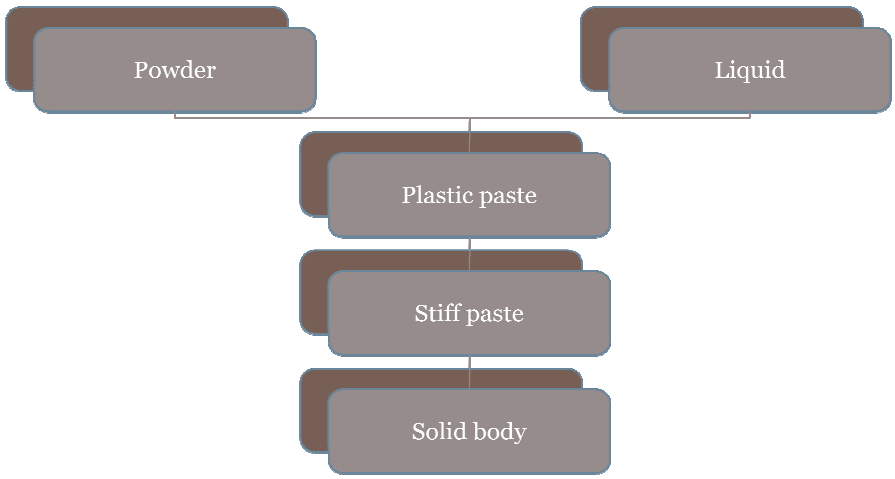

Fig. 4.13: Schema of the preparation of CPCs

Cements have to satisfy three different properties: first, the **setting time** –the time necessary from the moment in which the liquid and the powder are mixed to the moment when the cement is harden. It is the time required for the initial setting of the cement paste, which is reflected in a loss of plasticity. This time has to be contained between 4 and 8 minutes in case of clinical applications [31]. The cement must also maintain its **cohesion** when it gets in contact with an aqueous liquid. Finally, the cements must form

a castable paste, which can be easily moldable for a surgeon.

Because it has been reported that cements can sometimes have two hardening reaction, Driessens et al. [32] proposed to realize two measurements: the initial and final setting time. In order to measure the consistence of the paste, we used a manual method, to verify the ability of the paste to resist a mechanical load applied to its surface: the Gillmore needles.

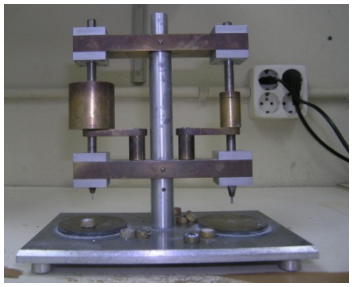

Fig. 4.14: the Gillmore needle

The initial setting time is measured using the light needle, and it indicates the end of mouldability without serious damage to the cement structure. The heaver and finer needle permits to determine the final setting time, when the cement can be touched and manipulated without damages.

Several parameters can be adjusted to have an adequate setting time. The main one is the liquid/powder ratio: the smaller amount of liquid, the shorter the initial setting time.

On the other hand, the cements are destined to be implanted into the human body, and so to be in contact with blood or other physiological fluids, while is still in a paste state. Hence their cohesion is a very important property. This property is evaluated by an immersion test. This consists on preparing the paste and introducing it in a brass mold. At the time that the cohesion need to be evaluated, the paste is removed from the mold and is introduced into an aqueous solution, the Ringer's solution (or water), that pretends be similar to the physiologic body fluids. The Ringer's solution is an aqueous solution with 0.9 wt % of NaCl.

Finally, the paste castability is evaluated while preparing the cements.

4.2.6.2. Advantages of CPCs

There are many reasons why the CPCs are widely used in orthopedic applications:

- Castable and injectable, allowing the minimal invasive surgery Setting is performed in vivo, and leads to a perfect adaptation to the bone cavity
- The reaction is non exothermic (being not harmful for cells)
- The reaction products are similar to biological HA (CDHA nanometric crystals)
- Products more resorbable than ceramic HA
- Biologically active molecules and drugs can be incorporated. It means that the cement have the ability to release some molecules with a certain control, which can be done with the porosity.

4.2.7. Advantages brought by silicon

Silicon is an essential trace element for bone growth which increases bioactivity (of α-TCP) and enhances cell proliferation. It is recognized [33-34] as having important effects on biological processes related to bone and connective tissue development. Bronner[7] suggests that it speeds up the bone mineralization process. Moreover, since it is a fundamental ingredient for the collagen, it is necessary for the formation and growing of bones, for both organic and inorganic phases.

Some studies [45-27] have focused on the preparation of Si-α-TCP, producing an exchanged between phosphor ions for silicon. There are no studies in which Si-doped cements are prepared, using a Si-CaP reactant. Nevertheless, a study written by Porter et al.[35] observes that when silicon ions are introduced into the HA structure, the apatite deposits morphology change: the collagen fibers are more evaluated in the Si-HA than in the HA.

Below is showed the phase diagram of the Ca_2SiO_4-$Ca_3(PO_4)_2$ system.

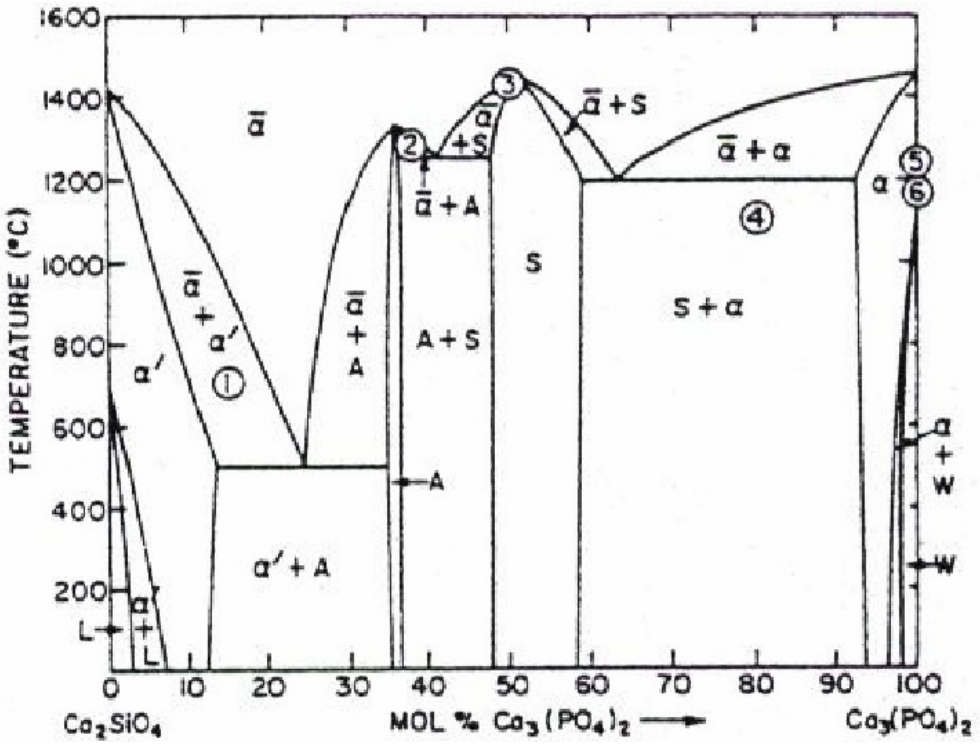

Figure 4.15: Phase diagram of the Ca_2SiO_4 - Ca_3PO_4 system (from Fix et al. [36])

Silicon stabilizes the α-phase at low temperatures. The phase-diagram indicates that in a Ca_2SiO_4-$Ca_3(PO_4)_2$ system, an α-phase can be obtained when there is 3 to 7 molar % of Ca_2SiO_4. Thereby, a quench seems to be not necessary to obtain this α-phase at room temperature. Moreover, it can be assumed that a less energetic thermal treatment could be probably used.

Having the knowledge that silicon ions substitute the phosphorous ones, to obtain a silicon doped TCP the Ca/(P+Si) ratio should be 1.5. It is possible to theoretically find the quantity silicon needed to fulfill this ratio.

It has been suggested [37] that a solid solution of α-TCP substituted with silicon, the Si-α-TCP, can be obtained from a mix of HA and SiO_2. Since phosphor and silicon ions have different electronic charges (P^{5+} and Si^{4+}), the final product created by these would contain defects in order to form a neutral product. The end-product will probably have both excess of calcium ions and defect of oxygen ions

4.2.8. LIMITS OF CALCIUM PHOSPHATE CEMENTS

The CPCs are a synthetic material which can implant themselves in a bone defect and help the regeneration of the material. Nevertheless, there are still two important limits nowadays:

- the in-vivo reasborption is not high enough [38]: it could be increased preparing a material which has a higher macroporosity (the osteoclasts are in direct contact with the cement and achieve the degradation) or a material whose crystallic cells are distorsioned [39]due to composition modification (to obtain a better solubility and so a faster degradation)
- the mechanical resistance is too low: one of the problems of the CPCs is that they only tolerate the compression forces and contrary to the bones or the teeth, they are more fragile and have a low resistance to impacts [40].

5. STATE OF THE ART

The superior biological performance of Si-HA and Si-TCP implant materials has been well documented [41,42,43,44,45]. For example, an in vivo study of CaP granules compares the biological activity of Si-HA with regard to HA, and reports an increase in bone in-growth of 14.5% in Si-HA versus HA controls[46].

Knowing the improved biological properties that can be provided by the introduction of silicon in calcium phosphate materials, recently, a few research groups have attempted to prepare components like Si-HA or Si-α-TCP. These materials have been mainly prepared by using wet chemical methods followed by sintering [47]. The wet chemical methods mainly comprise the sol-gel and precipitation. Nevertheless, these methods present some problems. Sayer et al. reported that in the precipitation method, it is difficult to control the stoichiometry [48].

The effect of the reactants on the wet chemical method has also been studied. It has been reported that the amount of impurities in the initial HA could influence on the phases formation[37].A more specific paper proves how Mg leads to form more β-TCP phase, in detrimental of the formation of α phase [45].

In general, the studies performed have prepared the HA, by sol-gel or precipitation, and have added silicon to the component formed in order to prepare HA or α-TCP doped with this element, after being a heat-treated. The Ca/(P+Si) atomic ratio has been proved to be very important to get closer to the CaP doped with silicon desired. Thus, in order to optimize the formation of this component, most of the papers evaluate the influence of the following parameters:

- Variation of the percentage of silicon introduced, and thus the Ca/(P+Si) atomic ratio
- Different heat treatments
- Different reactants
    - Considering the betagen effect of magnesium
    - Looking for the best silicon source to maximize the incorporation of this element into the end-product

So far, the best results reported obtain a single α-TCP phase by adding 0,87 wt% (0.16 SiO_2/HA molar ratio) by a wet chemical method followed by a heat-treated at 1250°C for 2h [49]. Although this result looks to be pretty good, the method employed is tedious, and the stoichiometry is difficult to control, being thus the reproducibility probably low.

From the results exposed in published studies, the information that is extracted is mainly that is very important:

(a) to consider the betagen impurities of the reactant, and
(b) to use a method which allows to control the stoichiometry of the end-product.

Using the knowledge obtained from the literature we will use a commercial betagen-free reactant as a source of Ca and P, and a milling method, which allows the control of stoichiometry.

6. MATERIAL AND METHODS

6.1. GENERAL OVERVIEW

The objective of this project is to obtain silicon doped calcium phosphate cements. To be able to prepare these cements, the process to achieve the Si-α-TCP powder must be optimized. The procedure of preparation has been divided in two main parts:

A) Preparation of Si-α-TCP
B) Preparation of calcium phosphate cements doped with silicon

A) Preparation of Si-α-TCP

The first goal is to prepare a Si-α-TCP powder. The two reactants used are: a calcium phosphate source, hydroxyapatite (HA), and a silicon source, silicon oxide (SiO_2, that we will refer as SO). In order to obtain the highest proportion of Si-α-TCP , a reactants mixture will be realized through a wet milling process using three different quantities of silicon, and will be followed by a sintering. In order to verify the effect of silicon, a control-powder without any silicon incorporated will also be prepared.

From the phase diagram, it is expected that when a CaP mixture with a Ca/P ratio of 1.5 is sintered, three different phases are formed: α-TCP, β-TCP and HA. Indeed, it was explained in the CaP section, that the α-phase is only formed when a thermal treatment is performed, since the β-phase is the one stable at room temperature. Nevertheless, silicon has the ability to stabilize the α-phase, and probably a less energetic treatment and/or less dramatic will be useful. Thereby, an important step will be the selection of an appropriate heat treatment to obtain a highly pure Si-α-TCP. Finally, the proportion of silicon chosen will be the one which give the higher amount of this phase.

B) Preparation of the CPC doped with silicon

Once the powder preparation method will be optimized, Si-α-TCP powder will be prepared, and it will be the powder phase for cements. The cements preparation consists on mixing Si-α-TCP with an aqueous liquid, being the phase hydrolyzed to transform into CDHA, according to the equation mentioned in the 4.2 6.1 section:

$$3\ \alpha\text{-}Ca_3(PO_4)_2 + H_2O \rightarrow Ca_9(HPO_4)(PO_4)_5(OH)$$

On the other hand, a cement-control will be as well prepared in order to compare the end-product formed with that one obtained when using silicon doped α-TCP. . This cement-control consist on using α-TCP as powder phase, which will be obtained by applying to HA (no mixed with silicon) the thermal treatment necessary in order to obtain the α-phase.

The following schema represents a general overview of the preparation process of the cements:

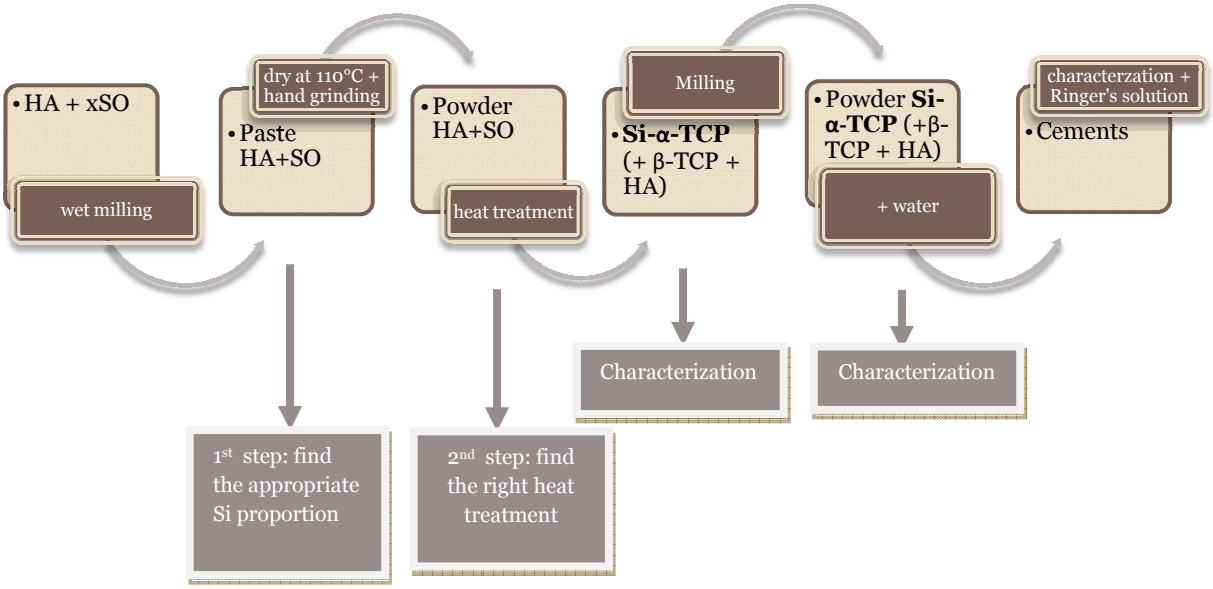

Figure 6.1: overview of the preparation process

6.2. THE REACTANTS

As mentioned previously, in order to prepare Si-α-TCP, we used the following reactants: a powder of Hydroxyapatite (Hydroxylapatite High Resolution CalbioChem Cat#391948 Lot#D00010693) that we will refer as **HA**; and a silicon dioxide in a form of colloidal aqueous dispersion (Cab-O-Sperse 1030K) in a proportion of 30% SiO_2/70% H_2O, we will refer as **SO**.

These two reactants have been chosen for several properties: their composition and their particle size. Indeed, we saw in the state of art section that the ideal hydroxyapatite should be free of betagens elements such as Mg, Sr, Al, Fe [57] and its surface area should be high, in order to get the closest contact with SO and facilitate the elements substitution. Moreover, this particle size should be small enough so that the cements have the best properties possible. The SO was also chosen for its particle size and its lack of impurities.

6.2.1. CHARACTERIZATION OF THE REACTANTS

Both reactants have been characterized by the following techniques:

Technique	Information
X-Ray Diffraction (XRD)	Phases proportion
Inductively Coupled Plasma (ICP) (optic and mass)	Impurities
Infra-Red Diffraction	Chemical bond of molecules
Transmission Electron Microscopy (TEM)	Particle morphology
Scanning Electron Microscopy (SEM)	Particle morphology
Granulometry	Particle size distribution
N_2 absorption (BET)	Specific surface

Table 6.1: Characterization techniques for the reactants

6.3. PREPARATION AND CHARACTERIZATION OF SI-α-TCP

6.3.1. THEORETICAL FUNDAMENTALS OF MILLING

In a mill, the reactants are crushed between balls or ball and wall (horizontal or planetary ball mill, attritor, vibratory ball mill), or between rings or ring and wall (multi-ring media mill). The mixture of the reactants is maximized, enhancing the close contact between them. Furthermore, the reactants could absorb part of the energy provided by the collisions or frictions that provide the energy necessary for the reaction. The milling can be performed under wet or dry conditions [50].

The grinding of solid matters occurs under exposure of mechanical forces that trench the structure by overcoming of the interior bonding forces. After the grinding the state of the solid is changed: the grain size, the grain size disposition and the grain shape. This way, the surface area of a solid is magnificated.

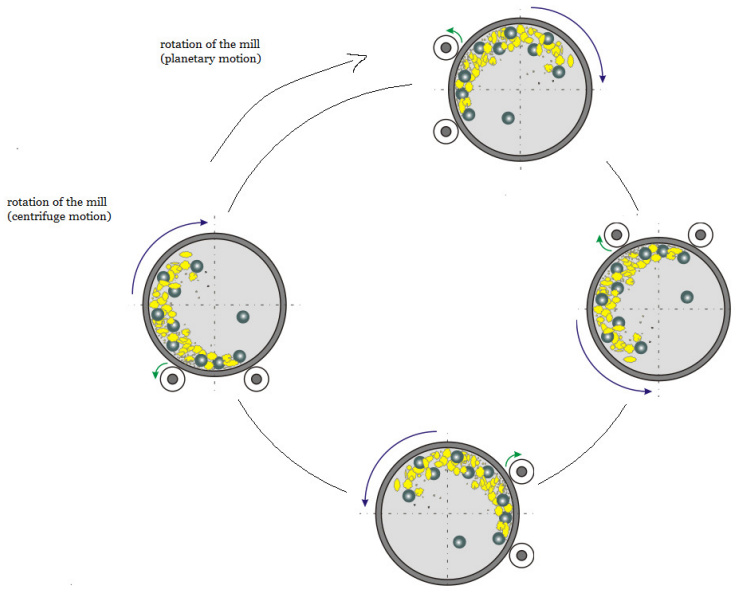

Fig 6.2: Schema of the milling process

The milling process is performed using conventional planetary milling balls for laboratory uses. Both the milling container and the balls are composed of agate.

The main drawback of the milling is the possible contamination of the samples with silicon, as a consequence of a partial deterioration of the mortar and the agate balls through the successive shocks. Agate is used since it is a quartz mineral with very high hardness. Therefore, the risk of contamination is quite low: if it deteriorates through the shocks during the grinding, the process would be very slow.

6.3.2. Preparation of Si-α-TCP

The process consists on milling the two reactants (HA and SO) with deionized water in an agate cylindrical mill container (volume capacity of 500 mL)

In order to check that the milling product has not been contaminated by the deterioration of the balls, a control of the balls was done before and after the milling process. This control consists on measuring the diameter and the weight of the agate balls. In the case to not see any significant difference it will be considered that o contamination has been produced. The Si-α-TCP is prepared from 20g of our HA to which the appropriate amount of SO is added. As we saw in our overview, three proportion of silicon will be tested.

6.3.2.1. CALCULATION OF THE THREE PROPORTIONS OF SILICON TO ADD

The goal is to obtain Si-α-TCP-phase after the grinding step and the application of a thermal treatment. We saw in the Calcium Phosphate chapter (4.2.5) that the appropriate Ca/(P+Si) atomic ratio to reach this phase is 1.5.

Thereby, knowing the chemical formula of our two reactants, we can find the right proportion of silicon to add (for the next calculations, it is assumed that the HA is stoichiometric):

HA ($Ca_5(PO_4)_3(OH)$) contains 5 atoms of carbon and 3 atoms of phosphor

SO ($SiO_2(H_2O)$) contains 1 atom of silicon

We are looking for x so that $\frac{(Ca)}{(P)+x(Si)} = 1.5$

The number of related atoms are: (Ca) = 5, (P) = 3 and (Si)=1,

The equation gives: **x~0.32**

This result give information of the theoretical ratio that the reactants should keep in order to produce Si-α-TCP: $Ca_5(PO_4)_3(OH) \cdot 0{,}32\ SiO_2(H_2O)$. In order to simplify, we will refer to this proportion as HA/SiO_2 in a 0.32 molar ratio.

However, this is only true if the HA used is perfectly stoichiometric. In order to cover a range of impurities, two other proportion close to the one found were tried: **x=0.16** and **x=0.48.** As we precised in the overview, a control is also realized, without SO.

6.3.2.2. CALCULATION OF THE AMOUNT OF SO NEEDED

Now that the three ratios that will be used are known, it has to be translated into weight and volume, so that the preparation can be performed.

Here below is the calculation made in order to get to know the mass of SO needed.

20g of HA are mixed with an unknown mass of SO

The molar weight respectively are M_{HA}=502.17 g/mol and M_{SO}=60.0632 g/mol

Knowing that the SO is dissolved in 30 wt % into water, the equation giving the mass needed is:

$$m = 20g Ca_5(PO_4)_3(OH) . \frac{1\ mol\ Ca_5(PO_4)_3(OH)}{502{,}17\ g/mol} . \frac{x\ mol\ SiO_2}{1\ mol\ Ca_5(PO_4)_3(OH)} . \frac{60{,}0633\ g\ SiO_2}{1\ mol\ SiO_2} . \frac{100g\ diss}{30\ g\ SiO_2}$$

Our four proportions are equivalent to:

x SiO_2·HA (molar)	Weight of SO to add (g)
0	0
0.16	1.2759
0.32	2.5517
0.48	3.8276

Table 6.2: weight of SO to insert to prepare the powder with the chosen amount of silicon

In order to weight with more precision and in an easier way, a correspondence between the volume and the weight of SO was performed. Since the density of the SO is not known, it has been approximately calculated, weighting different volumes of the suspension, and making a linear regression.

With an R^2=0.9999, the approximate density of the SO is 1.22 g/mL

Thereby, the amount of SO to add to the 20g of HA becomes:

x SiO_2·HA (molar)	Volume of SO to add (mL)
0	0
0.16	1.04
0.32	2.09
0.48	3.14

Table 6.3: volume of SO to insert to prepare the powders with the chosen amount of silicon

6.3.2.3. Experimental protocol

20g of HA are weighted and introduced into the mill ball.

In order to weight the SO with high accuracy, it was weighted inside an analytical balance with a saturated humidity environment.

The appropriate volume of SO is sonicated using 30mL of water. This preparation is added to the HA and 20mL more of water were used to quantitatively decant the SO dispersion. A spatula was employed to mix manually paste formed.

Inside the agate container are introduced 3 agate balls (ø=30mm). A grinding was performed in the planetary ball mill using a rotation speed of 350 rpm during 30 minutes.

Once the milling is made, our mixture was dried in an oven during 24h at 110°C. The powder obtained was manually ground using an agate mortar.

(a) (b) (c)

Fig 6.3: preparation of the powder: (a) agate milling container and ball, (b) planetary ball (c) agate mortar

6.3.3. HEAT TREATMENT

A) For Si-α-TCP optimization

The second step is to heat the powder in order to obtain Si-α-TCP.

According Sayer et al [48], the best heat treatment in order to obtain a maximum amount of α-phase is 1250°C during 2h, cooling the samples slowly inside the oven. Other heat treatments will also be tried: the suggested temperature will be used, but several dwell times will be tested (no dwell, 30 minutes, 2 hours).

B) For α-TCP optimization (control powder for the cements)

In parallel, the control powder for cements is also prepared. Since this powder does not contain silicon, the heat treatment has to be different: the temperature reached will not be the same, and maybe a quench will be necessary so that the α-phase is stabilized at room temperature. The aim will be to find the appropriate heat treatment.

The quench is performed in air, using a platinum molder.

Fig. 6.4: Photo of the quenching performed in air with the platinum molder.

6.3.4. Characterization of the Si-α-TCP

Before preparing the cements, the Si-α-TCP powder prepared was characterized in order to assure the quality of the future cement preparations.

Here are summarized the different characterization techniques that were used and the information that they provide:

Technique	Information
X-Ray Diffraction (Rietveld Refinement Method)	Phases proportion
Infra-Red Diffraction	Chemical bond of molecules
Scanning Electron Microscope (SEM)	Morphology
Transmission Electron Microscopy (TEM)	Morphology
N_2 absorption (BET)	Specific surface

Table 6.4: techniques used to characterize the powder after heat treatment

6.4. Preparation and characterization of cements

6.4.1. Grinding of the powder

In order to have an appropriate raw material for the preparation of cements, it is necessary to decrease the particle size of the Si-α-TCP, increasing then its reactivity. This was carried out by grinding together three batches of materials, corresponding to that SiO_2/HA molar ratio that was revealed to give a higher amount of Si-α-TCP.

The grinding was performed introduced 50 g of powder and 6 agate balls (ø=30mm). A

rotation speed 350 rpm during 30 min was applied.

Previously, the best SiO_2/HA proportion is chosen, i.e. the one which gave the more α-TCP. This powder is prepared three times in order to have 50g for the grinding.

6.4.2. CEMENTS PREPARATION

In order to adjust the setting and cohesion times of the cements, so that it fits into the usual clinical application range, the L/P ratio was adjusted. The liquid and the powder are mixed by hand in a glass mortar. The obtained paste is introduced into a brass cylinder and the setting is evaluated by pressing the surfaces with the Gillmore needle. A chronometer is running during this all operation and the time when the needle does not leave a mark on the paste is referred as the initial setting time. The cohesion time was also evaluated by immersing the cement in an aqueous liquid, and checking its integrity after 1 hour.

After several tries, it has been decided that the cements will have a Liquid/Powder ratio $\frac{L}{P} = 0.32$. It means that they are prepared from 1 mL of water and 3.125 g of the Si-α-TCP powder.

The cements are stored into Ringer's solution in an incubator at 37°C for different time: 8hours, 1 day, 3 days and 7 days.

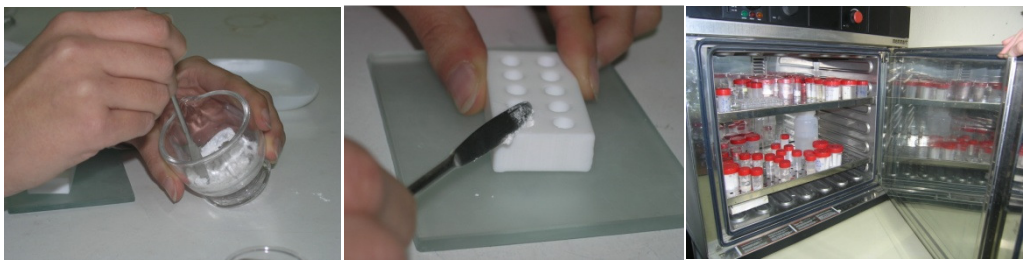

(a) (b) (c)

Fig. 6.5: preparation of the cements: (a) mixing the powder and liquid into a glass mortar, (b) introducing the paste into the cylinder mold (c) storing in simulated body fluid in the incubator

6.4.3. CHARACTERIZATION OF THE CEMENTS

The cements are characterized in order to evaluate the effect of silicon. Here are the characterization techniques used and the information they provide:

Technique	Information
X-Ray Diffraction (Rietveld Refinement Method)	Phases proportion
Infra-Red Spectroscopy	Chemical bond of the molecules
Scanning Electron microscope (SEM)	Particle morphology
Transmission electron microscopy (TEM)	Particle morphology
Granulometry	Particle size distribution
N_2 absorption (BET)	Specific surface
Mercury Intrusion Porosimetry (MIP)	Porosity / Bulk density / Pore size distribution
Pycnometry	Skeletal density
Universal machine for mechanical tests	Compression maximum

Table 6.5: Characterization techniques used for the cements

7. CHARACTERIZATION TECHNIQUES

The composition of the products prepared (crystalline phases) are evaluated by X-ray diffraction. This technique will be widely used in this project, in order to choose the best SiO_2 ratio and the appropriate heat treatment. Infra-Red spectroscopy also indicates the molecular groups formed, which gives information on the phase formed or the elements introduced into the lattice. Surface area, particle size and porosity are important characteristics, capable of affecting the quality and utility of many materials. At the same time they are important keys in understanding the structure, formation and potential applications of different natural materials. Information of the morphology of the reactants and products has been obtained from electronic microscopes (scanning and transmission). Finally, the mechanical properties of cements have been tested.

7.1. X-RAY DIFFRACTION

X-ray scattering techniques are a family of non-destructive analytical techniques which reveal information about the crystallographic structure, chemical composition, and physical properties of materials and thin films. These techniques are based on observing the scattered intensity of an X-ray beam hitting a sample as a function of incident and scattered angle, polarization, and wavelength or energy.

Powder diffraction (XRD) is a technique used to characterize the crystallographic structure, crystallite size (grain size), and preferred orientation in polycrystalline or powdered solid samples. Powder diffraction is commonly used to identify unknown substances, by comparing diffraction data against a database maintained by the International Centre for Diffraction Data. It may also be used to characterize heterogeneous solid mixtures to determine relative abundance of crystalline compounds and, when coupled with lattice refinement techniques, such as Rietveld refinement, can provide structural information on unknown materials.

When a monochromatic X-ray beam with wavelength λ is projected onto a crystalline material at an angle θ, diffraction occurs only when the distance traveled by the rays reflected from successive planes differs by a complete number n of wavelengths.

By varying the angle θ, the Bragg's Law conditions are satisfied by different d-spacings in polycrystalline materials. Plotting the angular positions and intensities of the resultant diffracted peaks of radiation produces a pattern, which is characteristic of the sample. Where a mixture of different phases is present, the resultant diffractogram is formed by addition of the individual patterns.

In this project, all the XRD results have first being evaluate qualitatively evaluating the most intense peaks of each phase, in order to have an overview of the proportion of the phases. Afterwards, the spectra were analyzed quantitatively with the Rietveld refinement method, method was that was developed by the Dutch crystallographer Hugo Rietveld.

The Rietveld method consists in simulating a diffractogram from a crystallographic model of the sample, then adjusting this model parameters in order to the simulated diffractogram could be the closest from the measured diffractogram. The parameters that were refined are the scale, the lattice parameters, the width at half height of the peak, etc. Thanks to the Rietveld method, the cells parameters can also be evaluated with a good precision.

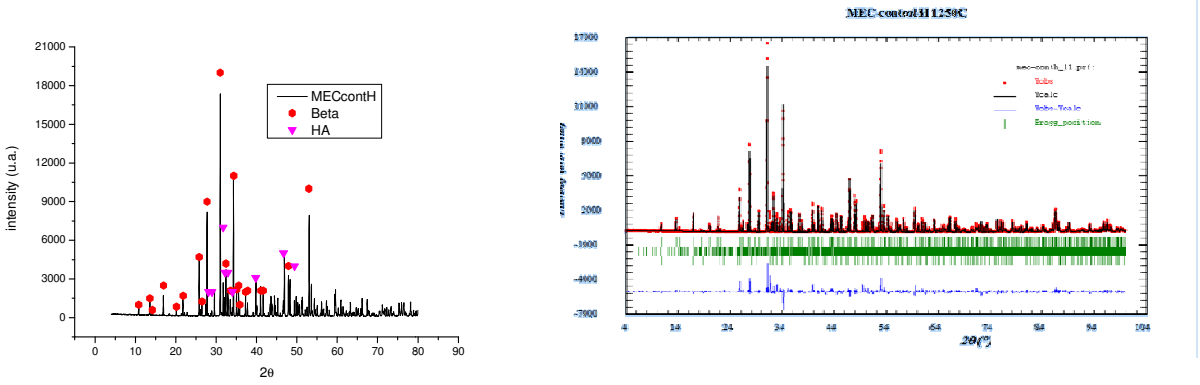

Fig. 7.1: Spectra obtained with Origin (qualitative analysis) and the Rietveld method (quantitative analysis)

The typical experimental conditions were: V = 45kV, I = 40mA, scan step 2θ = 0.02º, scan interval 4-100º and counting time of 150 s per point.

The phases present were qualitatively determined by high resolution XRD. Spectra were compared to PCPDFWIN, including spectra for α-TCP (PDF #09-0348) [51], β-TCP (PDF #09-0161) [52] and HA (PDF #09-0432) [53]. Rietveld refinements using FullProf software were carried on in order to quantify the phases present. In this case was used the Inorganic Crystal Structure Database (ICSD), including the spectra for α-TCP (ICSD #923) [54], β-TCP (ICSD #6191) [55] and HA (ICSD #151414) [56] Quality fits for phase quantification were obtained by refining the instrument displacement, scale factors, lattice

parameters using a Thompson-Cox-Hastinge pseudo Voight*Axial divergence, FWHM/shape parameters, preferred orientation and background. The Rietveld refinements were performed using the software package FullProf Suite [57] XRD spectra analyzed with Rietveld refinement were also used to calculate the lattice parameters of the constituent phases of each sample.

Fig 7.2: photo of the XRD machine

The XRD tests have been performed in the Scientifico-technic services of the University of Barcelona (SCT-UB) (Bragg-Brentano PANalytical X'Pert PRO MPD alpha1).

7.2. Inductively Coupled Plasma

An inductively coupled plasma (ICP) is a type of plasma source in which the energy is supplied by electrical currents which are produced by electromagnetic induction, that is, by time-varying magnetic fields.

A plasma is a gas that contains a sufficient concentration of ions and electrons to make the gas electrically conductive. In the plasmas used in spectrochemical analysis, the positive ions are almost all singly-charged and there are few negative ions, so there are nearly equal numbers of cations and anions in each unit volume of plasma.

ICP for spectrometry is sustained in a torch that consists of three concentric tubes, usually made of quartz. The end of this torch is placed inside an induction coil supplied with a radio-frequency electric current. A flow of argon gas is introduced between the two outermost tubes of the torch, and an electrical spark is applied for a short time to introduce free electrons into the gas stream. These electrons interact with the radio-frequency magnetic field of the induction coil and are accelerated first in one direction, then the other, as the field changes at high frequency. The accelerated electrons collide with argon atoms, and sometimes a collision causes an argon atom to part with one of its electrons. The released electron is in turn accelerated by the rapidly-changing magnetic field. The process continues until the rate of release of new electrons in collisions is

balanced by the rate of recombination of electrons with argon ions (atoms that have lost an electron). This produces a 'fireball' that consists mostly of argon atoms with a rather small fraction of free electrons and argon ions. The temperature of the plasma is very high, of the order of 10000 K.

The ICP can be retained in the quartz torch because the flow of gas between the two outermost tubes keeps the plasma away from the walls of the torch. A second flow of argon is usually introduced between the central tube and the intermediate tube to keep the plasma away from the end of the central tube. A third flow of gas is introduced into the central tube of the torch. This gas flow passes through the centre of the plasma, where it forms a channel that is cooler than the surrounding plasma but still much hotter than a chemical flame. Samples to be analyzed are introduced into this central channel, usually as a mist of liquid formed by passing the liquid sample into a nebulizer.

As a droplet of nebulized sample enters the central channel of the ICP, it evaporates and any solids that were dissolved in the liquid vaporize and then break down into atoms. At the temperatures prevailing in the plasma a significant proportion of the atoms of many chemical elements are ionized, each atom losing its most loosely-bound electron to form a singly charged ion.

In optic emission spectroscopy (OES), a sample solution is introduced into the core of ICP which generates temperature of approximately 8000°C. At this temperature all elements become thermally excited and emit light at their characteristic wavelengths. This light is collected by the spectrometer and passes through a diffraction grating that serves to resolve the light into a spectrum of its constituent wavelengths. Within the spectrometer, this diffracted light is then collected by wavelength and amplified to yield an intensity measurement that can be converted to an elemental concentration by comparison with calibration standards.

In ICP-MS (Mass Spectrometry) the ions from the plasma are extracted through a series of cones into a mass spectrometer, usually a quadrupole. The ions are separated on the basis of their mass-to-charge ratio and a detector receives an ion signal proportional to the concentration.

The concentration of a sample can be determined through calibration with elemental standards.

Both machines, ICP-OES and ICP-mass belongs to the SCP-UB (Thermo Jarrel Ash)

7.3. INFRARED SPECTROSCOPY

Infrared spectroscopy (IR spectroscopy) is the subset of spectroscopy that deals with the infrared region of the electromagnetic spectrum. The infrared region of the electromagnetic spectrum extends from 14,000 cm^{-1} to 10 cm^{-1}. The region of most interest for chemical analysis is the mid-infrared region (4,000 cm^{-1} to 400 cm^{-1}) which corresponds to changes in vibrational energies within molecules. The far infrared region (400 cm^{-1} to 10 cm^{-1}) is useful for molecules containing heavy atoms such as inorganic compounds, but requires rather specialized experimental techniques. It covers a range of techniques, the most common being a form of absorption spectroscopy.

The main goal of IR spectroscopic analysis is to determine the chemical functional groups in the sample. Different functional groups absorb characteristic frequencies of IR radiation. Using various sampling accessories, IR spectrometers can accept a wide range of sample types such as gases, liquids, and solids.

IR spectroscopy exploits the fact that molecules have specific frequencies at which they rotate or vibrate corresponding to discrete energy levels (vibrational modes). These resonant frequencies are determined by the shape of the molecular potential energy surfaces, the masses of the atoms, and by the associated vibronic coupling. In order for a vibrational mode in a molecule to be IR active, it must be associated with changes in the permanent dipole. Thus, the frequency of the vibrations can be associated with a particular bond type.

Simple diatomic molecules have only one bond, which may stretch. More complex molecules have many bonds, and vibrations can be conjugated, leading to infrared absorptions at characteristic frequencies that may be related to chemical groups.

IR spectra are obtained by detecting changes in transmittance (or absorption) intensity as a function of frequency. Most commercial instruments separate and measure IR radiation using dispersive spectrometers or Fourier transform spectrometers.

This technique works almost exclusively on samples with covalent bonds. Simple spectra are obtained from samples with few IR active bonds and high levels of purity. More complex molecular structures lead to more absorption bands and more complex spectra.

Fig. 7.3: photo of the IR spectroscopy machine

The IR spectra have been realized in the Materials Sciences and Metallurgy Engineering Department of the ETSEIAT, Terrasa (Nicolet 6700, software OMNIC).

7.4. Scanning Electron Microscopy

The Scanning Electron Microscope (SEM) is a microscope that uses electrons rather than light to form an image of the sample. It has a wide field depth, and this way a big part of the sample can be focused simultaneously. Since the SEM uses electrons to produce an image, most conventional SEMs require that the samples be electrically conductive. The SEM which is in the Materials Science Department of UPC, requires a conductive sample. All metals are conductive and require no preparation to be viewed using an SEM. In order to view non-conductive samples such as cements, the sample must be covered with a thin layer of a conductive material.

In SEM, an electron beam is thermally emitted from an electron gun fitted with a tungsten filament cathode (used for its low cost). The electron beam, which typically has an energy ranging from a few hundred eV to 40 keV, is focused by one or two condenser lenses to a spot about 0.4 nm to 5 nm in diameter. The beam passes through pairs of scanning coils or pairs of deflector plates in the electron column, typically in the final lens, which deflect the beam in the x and y axes so that it scans in a raster fashion over a rectangular area of the sample surface.

When the primary electron beam interacts with the sample, the electrons lose energy by repeated random scattering and absorption within a teardrop-shaped volume of the specimen known as the interaction volume, which extends from less than 100 nm to around 5 μm into the surface. The size of the interaction volume depends on the electron's landing energy, the atomic number of the specimen and the specimen's density. The energy exchanged between the electron beam and the sample results in the reflection of high-energy electrons by elastic scattering, emission of secondary electrons by inelastic

scattering and the emission of electromagnetic radiation, each of which can be detected by specialized detectors. The beam current absorbed by the specimen can also be detected and used to create images of the distribution of the specimen.

Electronic amplifiers of various types are used to amplify the signals which are displayed as variations in brightness on a cathode ray tube (CRT). The raster scanning of the CRT display is synchronized with that of the beam on the specimen in the microscope, and the resulting image is therefore a distribution map of the intensity of the signal being emitted from the scanned area of the specimen.

Then the image is digitally captured and displayed on a computer.

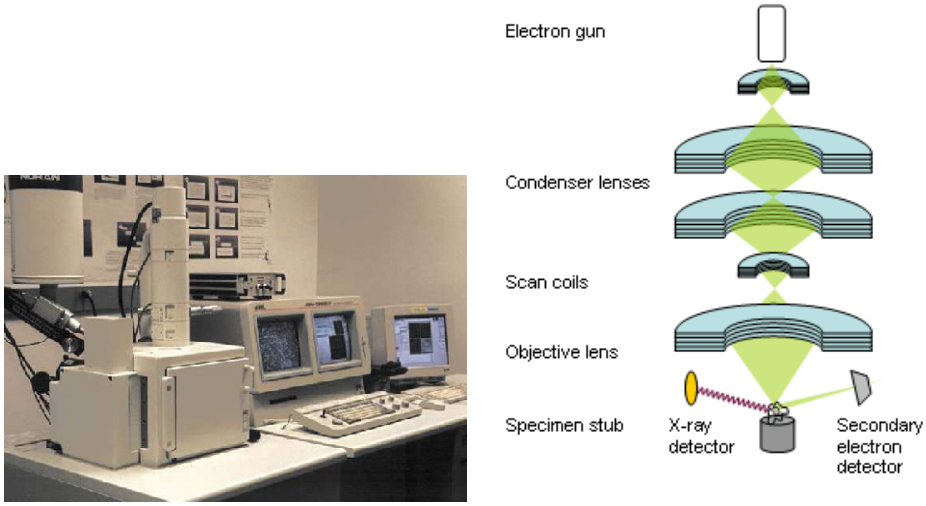

Fig. 7.4: photo of the SEM and schema of its functioning

7.5. Transmission Electron Microscopy

The first transmission electron microscopy (TEM) was built by Max Knoll and Ernst Ruska in 1931, with this group developing the first TEM with resolving power greater than that of light in 1933 and the first commercial TEM in 1939.

TEM is a microscopy technique whereby a beam of electrons is transmitted through an ultra thin specimen, interacting with the specimen as they pass through. The TEM operates on the same basic principles as the light microscope but uses electrons instead of light, since what we can see with a light microscope is limited by the wavelength of light.

TEM uses electrons as "light source" and their much lower wavelength make it possible to get a resolution a thousand times better than with a light microscope. An image is formed from the interaction of the electrons transmitted through the specimen, which is magnified and focused onto an imaging device, on a layer of photographic film.

TEMs are capable of imaging at a significantly higher resolution than light microscopes, owing to the small de Broglie wavelength of electrons. This enable the instrument to be able to examine fine detail – even as small as a single column of atoms, which is tens of thousands times smaller than the smallest resolvable object in a light microscope.

A "light source" at the top of the microscope emits the electrons that travel through vacuum in the column of the microscope. Instead of glass lenses focusing the light in the light microscope, the TEM uses electromagnetic lenses to focus the electrons into a very thin beam. The electron beam then travels through the specimen you want to study. Depending on the density of the material present, some of the electrons are scattered and disappear from the beam. At the bottom of the microscope the unscattered electrons hit a fluorescent screen, which gives rise to a "shadow image" of the specimen with its different parts displayed in varied darkness according to their density. The image can be studied directly by the operator or photographed with a camera.

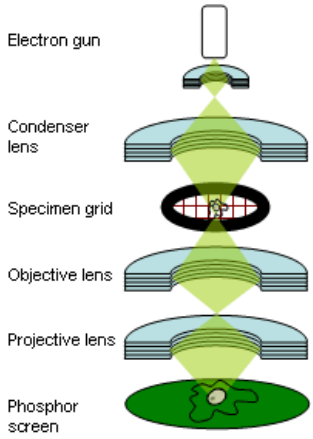

Figure 7.5: Schema of TEM

TEM forms a major analysis method in a range of scientific fields, in both physical and biological sciences. TEMs find application in cancer research, virology, materials science as well as pollution and semiconductor research. At smaller magnifications TEM image

contrast is due absorption of electrons in the material, due to the thickness and composition of the material. At higher magnifications complex wave interactions modulate the intensity of the image, requiring expert analysis of observed images. Alternate modes of use allow for the TEM to observe modulations in chemical identity, crystal orientation, electronic structure and sample induced electron phase shift as well as the regular absorption based imaging.

Once the images to be analyzed have been selected, the negatives have been printed and then developed into the laboratory of the department. Then, they have been scanned in the Scientific Park of Barcelona (Artix Scan 2500f, Microtek – Scanwizard Pro).

7.6. LASER GRANULOMETRY

Since the particle size of a cement powder influences its reactivity [58-59], the laser granulometry had been used. It measures the size of particles, or more precisely their diffraction of rays, thus making it possible to determine their grain size frequency. The measuring range is between 0.04 and 2000µm, making the laser granulometer particularly useful for polymer solutions and all kinds of mineral powders.

Laser granulometry uses the principle of light diffraction. It is based on the Fraunhofer theory, which makes the following assumptions:

- the particles are spherical, non porous and opaque (to be able to reflect the light)
- the particle diameter is greater than the wavelength of the light beam
- the particles are spaced enough one to another
- the particles have a random motion
- the particles diffract light with the same efficiency, whatever their size

A diffraction pattern is obtained when a laser beam strikes a particle. According to the theory, the intensity of the diffracted rays and the angle of diffraction are functions of particle size. The larger the particle, the more it scatters light, and the smaller the angle of refraction. However, the above theory is limited in its application as it applies only to particles of diameters larger than the wavelength of the incident light.

In order to analyze the powder, it is important to disperse (and not dissolve) the powder. The dispersion has been made with ethanol.

Fig. 7.6: photo of the granulometry machine

The machine used for the laser granulometry characterization belongs to the SCT-UB, in the Modular building (LS 13 320 Beckman Coulter).

7.7. NITROGEN ABSORPTION

The most widely used technique for estimating surface area (also the one we use) is the so-called BET method (after the initials of the inventors of this type of analysis: Brunauer, Emmett and Teller, 1938 [60]). This technique is based on a particular equation that allows determining a parameter of great importance in the study of the solid ones that is the superficial specific area (SS). Such parameter expresses the relationship between the total surface of the catalyst and the weight of the same one and usually is expressed in m^2/g (meters squared of surface on gram of catalyst).

The first step of the experiment is to do a complete degasification of the sample (the vapor molecules which are adsorbed into the material). This way, the characterization starts with a net superficial area. Then, the Nitrogen introduces itself in the system, so that one part of it is adsorbed and the rest stay in a gas state. Once the equilibrium is obtained and that the amount of adsorbed molecules is known, the pressure raises slowly until the material cannot adsorb more gas molecule in its superficial area [61].

The BET technique uses the principle of the physical inert gas adsorption and can be carried in static or dynamic conditions.

Figure 7.7: photo of the BET machine

The BET machine used belongs to the Biomaterials group in the Materials Sciences and Metallurgy Engineering Department of the ETSEIB (ASAP 2020, Micromeritics).

7.8. HELIUM PYCNOMETER

Helium pycnometry is used to determine skeletal density of a solid material with microporosity and gives indirect information about pore volume and closed porosity.

Samples are analyzed by a gas displacement pycnometer, which measures the volume of solid objects of irregular or regular shape, whether powdered or in various pieces. Helium is used as a displacement medium. The sample is sealed in the instrument compartment, helium is admitted, and then expanded into another precision internal volume. The pressure before and after expansion is measured and is used to compute the sample volume. The helium displacement density is obtained when dividing the volume by the sample weight. The samples are disposed in chambers of 1 or 3.5 cm^3, according to their size (in our case 1 cm^3).

fig 7.8: photo of the AccuPyc 1330 Pycnometer

The pycnometer used belongs to the Biomaterials group in the Materials Sciences and Metallurgy Engineering Department of the ETSEIB (AccuPyc 1330 Pycnometer Micromeritics).

7.9. Mercury Intrusion Porosimetry

Mercury Intrusion Porosimetry (MIP) is a technique used to measure pore size distribution. It is able to span the measurement of pore sizes ranging from nanometers to several hundred micrometers. This technique provides detailed information on pore volumes, density, and pore-specific surface area, while also yielding information that can be used to characterize the shape and structure of pores. The total volume of interparticular pores depends of the shape and size of each particle and also varies whether they are compacted or not [62].

In the MIP method, mercury is forced to penetrate into porous samples under stringently controlled pressures: various levels of pressure are applied to a sample immersed in mercury (a non wetting liquid). Intrusion is not instantaneous; mercury begins entering a pore opening at the moment the pressure exceeds the value required for the pore opening's diameter, but the time required for the mercury to fill the pore is dependent upon its volume and shape. The equilibration mode of operation holds pressure steady while the pores fill. Depending on the extent of equilibration the user specifies, pore volume readings taken using this type of analysis show the complete pore volumes. If equilibration is not allowed, filling may be incomplete when the instrument takes the volume reading, then moves on to the next pressure point.

Determination of the pore size by mercury penetration is based on the behavior of non-wetting liquids in capillaries. A liquid cannot spontaneously enter a small pore which has a wetting angle of more than 90 degrees because of the surface tension (capillary depression). However this resistance may be overcome by exerting a certain external pressure. The pressure required is a function of the pore size, the relationship between the pore size exerted when the pore is considered to be cylindrical, is expressed as:

$$pr = 2s \cos(q)$$

where r = pore radius.
s = surface tension of mercury.
q = contact angle (wetting angle).
p = absolute pressure exerted.

The results obtained from the instrument are: the pore size distribution (macro/meso range of porosity spectrum), the hysteresis curve, the specific surface, the bulk density, the

total porosity (%) and the particle size distribution.

Fig. 7.9: photo of the MIP

The MIP used belongs to the Biomaterials group and is located in the Materials Sciences and Metallurgy Engineering Department of the ETSEIB (Autopore IV 9500).

7.10. MECHANICAL TESTS

The cements have been mechanically tested with a universal testing machine. In order to evaluate their resistance to compression, all the samples were tested under a load of 10kN and a compression velocity of 1mm/s. The cements tested are cylinders with the following dimensions: h=12mm, d=6mm

From the mechanical properties obtained, the Young elastic modulus has been calculated:

$$E = \frac{stress}{strain} = \frac{\sigma}{\varepsilon} = \frac{F/S}{L - L_0}$$

with $\sigma=F/S$ the strength (F the force and S the surface) and $\varepsilon=(L-L_o)/L_o$ the deformation (L_o the initial length or highness).

Fig. 7.10: picture of the universal test machine Adamel Lhomargy DY 32/34

The universal testing machine used belongs to both investigation groups "Polymers and Composites Technology" and Biomaterials in the Material Sciences and Metallurgic Engineering of the ETSEIB (Adamel Lhomargy DY 32/34, software AUTOTRAC).

8. RESULTS AND DISCUSSION

8.1. REACTANTS

The aim here was not only to evaluate and discuss the phases and particles size of our reactants, but also to check on the impurities:

8.1.1. PHASES AND IMPURITIES PRESENT IN THE REACTANTS

The first step was to characterize the reactants by XRD in order to evaluate their possible impurities on other phases Here are the XRD spectra obtained:

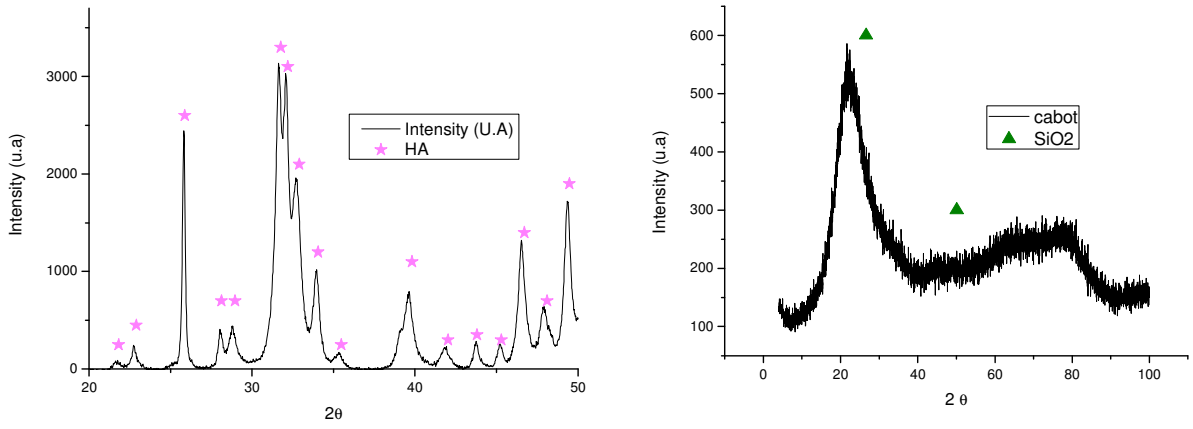

(a) (b)

Fig 8.1: XRD spectra of the reactants – (a): HA with characteristics peaks indicated, (b): dry SO with characteristics SiO_2 peaks indicated

As it can be seen, the HA is a crystalline phase with other crystalline phases. The spectrum of SO is formed for two wide peaks, indicating that this is an amorphous component, due mainly to its small particle size (see 8.1.2.2 section).

The HA was also characterized by ICP in order to know the impurities that contains, and its real Ca/P ratio. The samples were prepared by dissolving the HA in milli-Q water, with a 2wt % of HCl. Three replicas of the HA solution and three blanks have been analyzed.

The ICP-OES gave a Ca/P ratio of **1.43** instead of the 1.67 expected in case of a stoichiometric HA. It means that for the SiO_2/HA molar ratio of 0.48 that has been selected, the Ca/(P+Si) ratio also changes, and become: $\frac{Ca}{P+Si} = 1.43 \times \frac{1.5}{1.67} = \mathbf{1.28}$

In the following table are summarized the elements found into the HA, using both techniques of ICP, OES detector for K, Na, Si and Fe) and MS detector for Mg, Sr, Al, Mn, Cu and Zn:

(ppm)	Mg	Sr	Al	Fe	Na	Si	Mn	Cu	Zn	K
HA	9.38	49.12	5.71	34.24	**16713.23**	6.49	0.41	14.08	176.31	0

Table 8.1: impurities presents into the HA, as measured by ICP-OES and ICP-MS in ppm (mg of the element contained in 1 kg of HA)

Mg, Sr, Al and Fe are betagen elements. Nevertheless, they are found in a low concentration, lower than 10 ppm (10 mg of element impurity/Kg of HA) in the case of Mg and Al, and lower than 40 ppm in the case of Sr and Fe. In fact, by the β to α transformation, the element that has been more widely reported to act as β stabilizer is Mg, which concentration is pretty insignificant.

On the other hand, sodium is found in a high concentration, which will imply two different things:

- Na can stabilize the α-phase, as its ability to act as alphagen element when is present in high concentration has been reported by Ando [63]
- It is probably occupying calcium sites. This fact could explain the low Ca/P ratio of the HA, and also its low thermal stability at high temperature.

Considering then that the Na is occupying Ca sites, the (Ca+Na)/P ratio of the initial HA is 1.51, which is not that far to a stoichiometric HA (Ca/P = 1.67). This fact partially enlightens how Si-α-TCP can be obtained although the initial calculus were done considering a stoichiometric HA (see further explanation in the 8.2.1 section).

Thus, new calculations of the Ca/P ratio of the HA can be made, considering that sodium is occupying calcium sites. In the following tables are calculated these new ratios:

$SiO_2/_sHA$	Ca/(P+Si)	(Ca+Na)/(P+Si)
0	1.43	1.51
0.16	1.35	1.44
0.32	1.29	1.36
0.48	1.23	1.30

Table 8.2: Ca/P atomic ratio of the HA considering the impurities

Finally, the reactants have been characterized by FTIR. The following figure shows the FTIR spectrum and the corresponding bands of the reactants: HA and SO. The bands have been indicated on the spectrum, being all of them typical of each reactant.

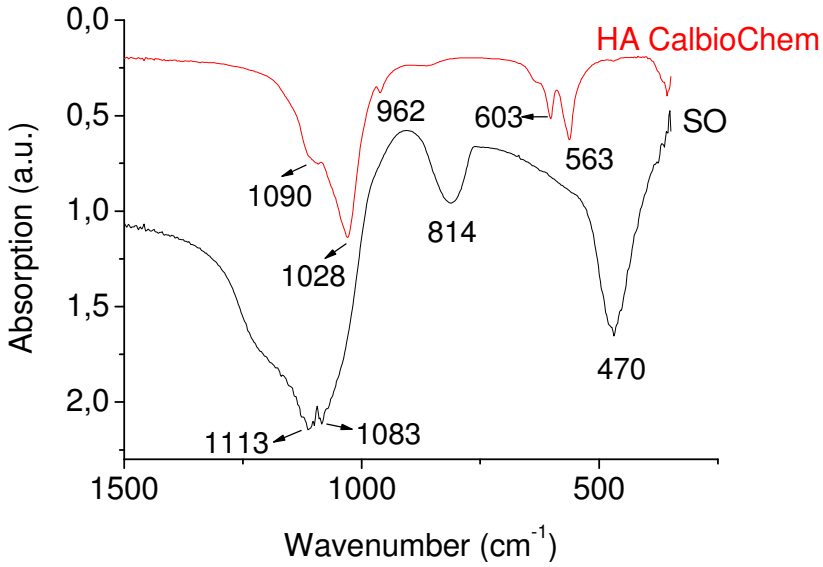

Fig. 8.2: IR spectrum of the reactants

The following tables indicate the most relevant bands found experimentally and those that have been previously reported by other authors, for both reactants.

(cm^{-1})	HA exp	HA [64-65-66]
ν_1 Sym. P-O stretch	962	962
ν_2 O-P-O bending	563	565
ν_3 Asym. P-O stretch	1090	1090
ν_4 Asym. P-O bend	563	565

(cm^{-1})	SO exp	SO [67]
ν_2 O-P-O bend	470	459
Si-O-Si bend of a thermal SiO_2 layer	814	814
	1083	1085
	1113	

Table 8.2: experimental and most expected bands of FTIR of HA and SO

The experimental spectra of both reactants are very similar to the peaks expected from Sayer et al. [64-67].

8.1.2. Particle size

8.1.2.1. Hydroxyapatite

In the following section the results obtained with several characterization techniques will be compared. The following pictures were taken by the SEM and give information on the morphology of HA:

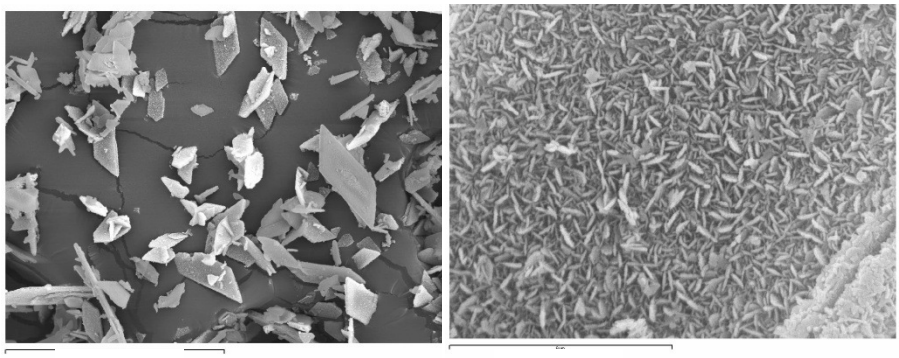

Fig. 8.3: HA CalbioChem by SEM: (a) x3000 and (b) x10000

The particles have a romoedric shape with a particle size range between 17 and 52 µm. It is important to notice that there are many nanocrystals on the surface of particles, increasing

significantly the rough morphology of this reactant. Thereby, the specific surface area of the hydroxyapatite is high: 70.68 (±0.07) m^2/g.

Granulometry gives us a range of the particle size of the reactant: between 14.16 and 48.40 µm. This result coincides with the calculated from the SEM picture.

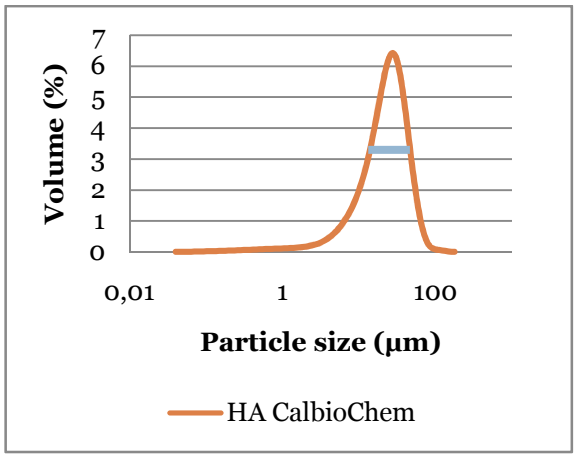

Fig. 8.4: particle size of HA given by granulometry; with a mean size between 14.25 and 48.70 µm

8.1.2.2. SO (Silicon Oxide)

A similar study was performed to evaluate the morphology of the SO. The morphology of this reactant was evaluated using TEM, as this microscope allows the obtaining of particles at nanometric sizes.

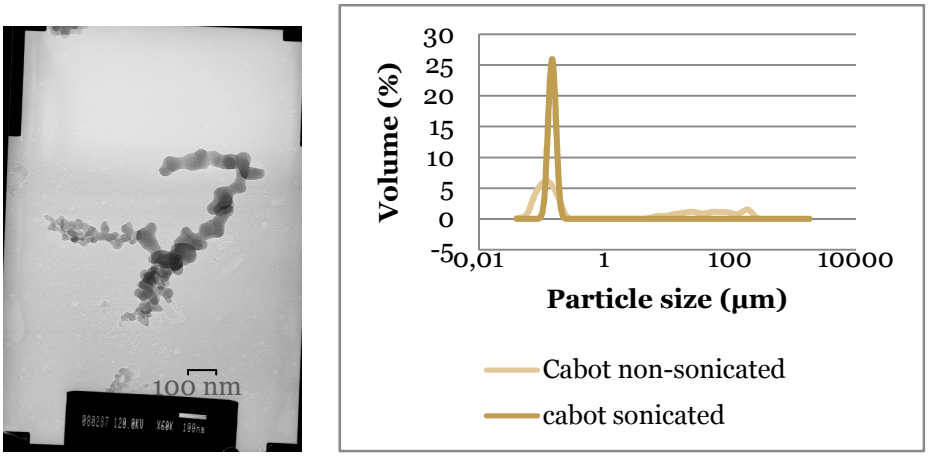

(a) (b)

Fig. 8.5: Characterization of SO: (a) by TEM (b) by granulometry. The mean particle size is between 12 and 20 nm.

The image obtained by TEM show a high compaction of the particles, revealed for darker zones. Nevertheless, is possible to appreciate a round morphology of the particles, with sizes between 12.10 and 20.25 nm.

Comparing the TEM micrograph with the curve obtained by granulometry, the size of the particles is similar. The mean size calculated by granulometry gives a range of 12.25-16.95 nm. The granulometry results also show clearly the importance of the sonication step for the SiO_2 dispersion (SO): the particle size distribution is indeed better defined since there are less agglomerate.

Finally, the specific surface area of the SO is 73.01 ±0.41 m^2/g. This high value was expected since the SO is composed with many small particles, giving place to a high surface area.

The particle sizes of the HA and SO are quite different, although their specific surface is pretty similar. This can be explained by their morphology, as previously said. The specific surface of the HA is high because of the nanocrystals, raising the global area of particles, and the important specific surface of the SO is explained by the small size of its particles. It is a real advantage to have such a high specific area, because the mixing will be better, the reactants will be in close contact and their interaction will be improved.

8.2. Preparation and characterization of the powder

8.2.1. Influence of silicon – wet milling

With the aim to obtain Si-α-TCP powder with high purity, the powder has been prepared as described in the "Material and Methods" section and heat treated at 1250°C. In order to evaluate the silicon incorporation into the α-TCP lattice, the crystalline phases formed have been quantified by XRD, using the Rietveld refinement method. .

The following graph shows the phases repartition, according to the proportion of silicon introduced (represented in SiO_2/HA molar ratio, considering a stoichiometric HA).

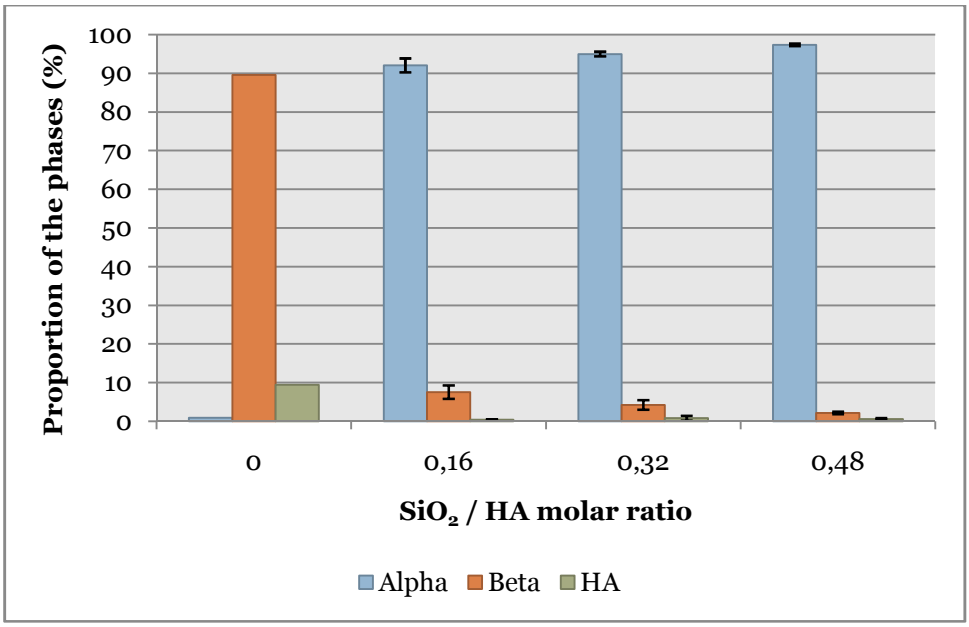

Fig. 8.6: the three crystalline phases repartition according to SiO_2/HA molar ratio

The first important remark is that the silicon introduced clearly has an effect on the phases formed. While the control powder (no silicon added, 0 SiO_2/HA) is almost only composed by β-TCP, when silicon have been added to HA, the proportion of α-phase is pretty high. These results are coherent with the phase diagram in the 5.5 section. The β-phase is formed in the case of no silicon addition, because this is the phase stable at room temperature. The proportion of crystalline phases formed also indicates that, in the chosen preparation conditions, the more silicon introduced, the more α-TCP is obtained.

Theory suggested that the best reactants ratio in order to optimize the α-phase formation would be 0.32 SiO_2/HA molar ratio, considering a stoichiometric HA, and supposing that all the silicon atoms of SiO_2 substitutes the phosphor ones in the HA. However, might be that not all the silicon atoms added are incorporated into the HA, being then necessary to introduce an excess of this reactant in order to enhance this substitution.

The excess of SiO_2 favors the reaction in two different ways: the silicon does not stoichiometricaly limit the achievement of the reaction, and a higher quantity of the SO also improves the contact between the two reactants. As a consequence, 0.32 SiO_2/HA molar ratio does not give as much as α-TCP as expected. Nevertheless, the Si-α-TCP is almost pure when a 0.48 SiO_2/HA molar ratio is used (more than 97 wt% of Si-α-TCP according to the Rietveld refinement method).

Focusing on the SiO_2/HA molar ratio of 0.48, it seems to be unexpected to reach such a high α-TCP amount since the Ca/(P+Si) atomic ratio is significantly inferior than 1.5, precisely being 1.23. However, as explained previously (9.1.1 section), it might be explained by the substitutions of calcium by sodium of the initial HA. Moreover, if we consider that not all of the SiO_2 added react with the HA but only a part of them are introduced into the lattice (might be less than 0.16 SiO_2/HA molar ratio), the (Ca+Na)/(P+Si) reached is probably can be to a 1.5 ratio.

In conclusion, the proportion chosen to obtain Si-α-TCP is **0.48 SiO_2/HA ratio**. From now on, the powder will be prepared according to this ratio, and so will be the corresponding cements

The influence of the silicon introduced has also been observed on other criteria: the specific surface area, calculated with the Nitrogen absorption characterization technique. Here behind is showed a graph of the impact of the reactants mixed after having been calcined at 1250°C

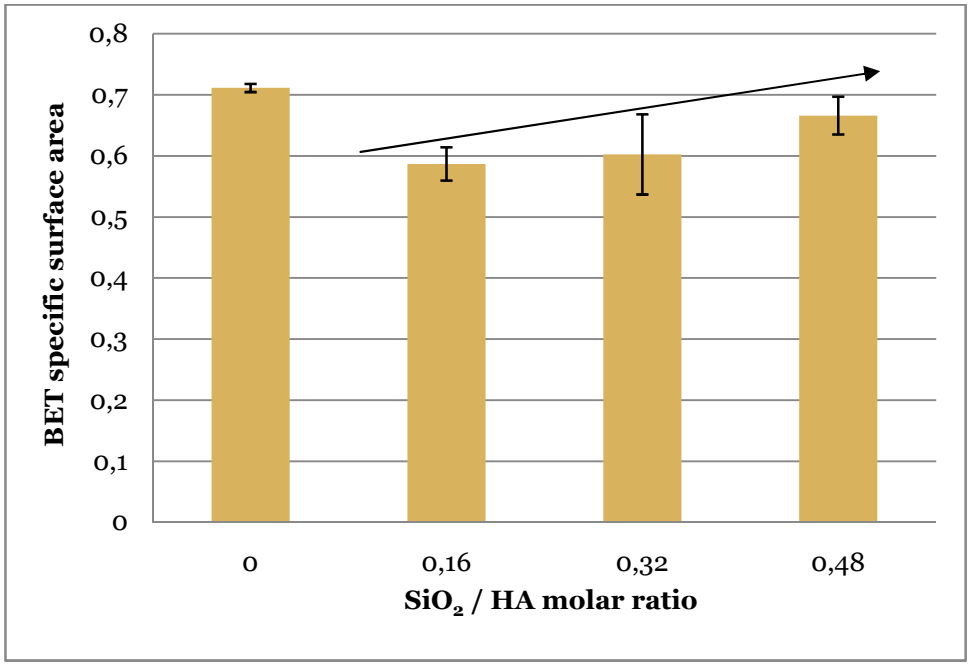

Fig. 8.7: influence of the silicon introduction on the specific surface area of the powder.

In this graph is observed that, the more silicon is introduced, the bigger is the specific surface area of the powder. Although the standard deviation indicates that the raise is not significant, the mean values show a slight increase on the specific surface area while introducing silicon.

The specific surface areas are measured after the thermal treatment. Thereby, it is expected that the SO particles and HA mixed have sintered. Since the graph above shows that the higher addition of SO increases the specific surface area, it means that this property is mainly dominated by this component, even after the thermal treatment. The specific surface area of initial HA has probably decreased drastically because its high value on this property was due to nanometric crystals easily sinterable. Moreover, it has now transformed into α-TCP.

Moreover, this specific surface area increasing can also be due to a residual excess of SO. Nevertheless, it is important to precise that the small values obtained are in the limit of sensibility of the nitrogen adsorption characterization technique.

Finally, it can also be noticed that, the surface area of the control powder is higher than the one when silicon is introduced. These results are not comparable with those explained previously since the crystalline phases present into the control powder are not the same: instead of measuring the specific surface area of α-TCP, this powder is composed by β-TCP and HA.

8.2.1.1 Characterization of Si-α-TCP and comparison with α-TCP

The introduction of silicon has also been observed through IR spectroscopy. The spectrum and some of the more significant bands, for α-TCP and Si-α-TCP (the values found experimentally compared with those reported in the literature) are displayed below:

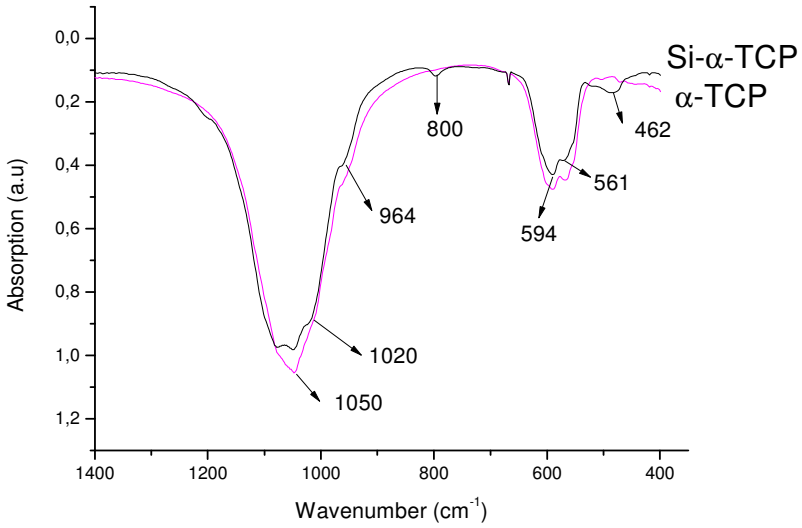

Fig 8.8: IR spectra of Si-α-TCP and α-TCP powder

Band (cm^{-1})	α-TCP (cm^{-1})	α-TCP [68] (cm^{-1})	Si-α-TCP (cm^{-1})	Si-TCP [68] (cm^{-1})
ν_1 Sym. P-O stretch	959	957	964	964
ν_2 O-P-O bending	471	450	462	459
	565	559	561	567
	589	589	594	592
ν_3 Asym. P-O stretch	1020	1009	1020	1015
	1044	1044	1050	1044

Table 8.3: Table of the main bands of the Si-α-TCP, grouped by their vibration type

Referring to α-TCP, some differences are found with those peaks related in literature [68]. The peaks corresponding to Si-α-TCP observed on the spectrum are close to those predicted by theoretical values or reported by other authors for Si-stabilized-α-TCP [68].

Comparing the bands of α-TCP with those obtained when silicon is introduced into the lattice, a shift is observed in some of the bands. The symmetric P-O stretch bands are approximately maintained at the same frequency; in the case of O-P-O bending the bands are shifted from 471 cm^{-1} to 462 cm^{-1}, from 565cm^{-1} to 561 cm^{-1} and also 589 cm^{-1} to 594 cm^{-1}. Finally, it is observed that the bands corresponding to the asymmetric P-O stretch are also shifted from 1044 cm^{-1} to 1050 cm^{-1}).

Finally, it was noticed that at 800 cm^{-1} appears a band which has been reported to belong to nanometric SiO_2 [49, 69]. This band confirms the fact that the crystalline end-product also contains the excess of SiO_2, although the SO used shows this band at 814cm^{-1}. This excess of SiO_2 probably screens the incorporation of silicon into the lattice, which would be revealed for the Si-O vibration of the silicate group formed into the Si-α-TCP.

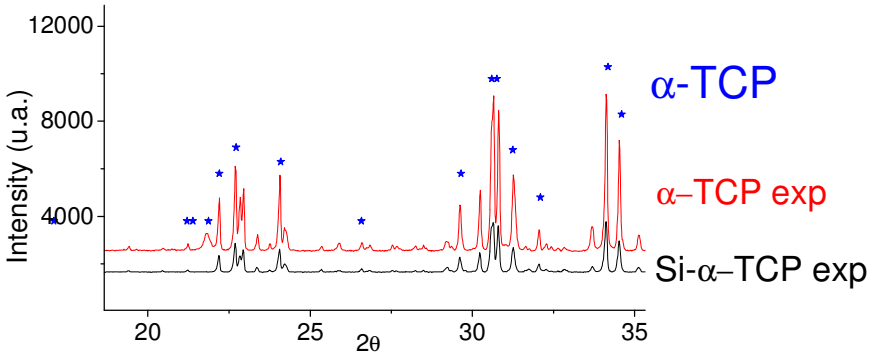

Fig 8.9: comparison between the spectra of α-TCP and Si-α-TCP

The peaks of XRD spectrum are the same for both α-TCP components, independently of the silicon addition. Nevertheless, its peak height is different, what might indicate a difference on the crystallinity of the phases. The α-TCP seems to be more crystalline.

8.2.2. Heat treatment Influence

As seen in the general overview, the second important step of the project was to find the right heat treatment for both preparations: Si-α-TCP and α-TCP (the control powder). Both powders will be used for the preparation of cements.

A) Preparation of Si-α-TCP

Sayer et al. suggested that the best thermal treatment to obtain a highly pure Si-α-TCP was to raise the temperature until 1250°C during 2 hours [49]. Nevertheless, in this work were also tried other heat treatments, in order to check if there was a more economic manner to obtain the wanted product. These tests were realized using a powder prepared with a 0.48 SiO_2/HA molar ratio.

The graphic below shows the phases repartition obtained when a temperature of 1250°C was applied, for several dwellings:

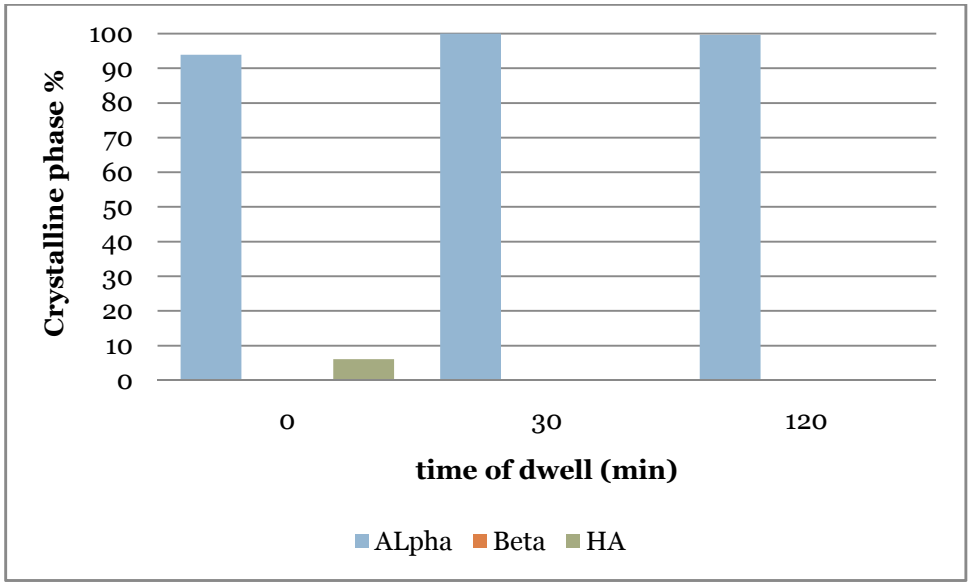

Fig. 8.10: influence of dwell time (no dwell, 30 min and 2 hours) on the crystalline phases formed

The XRD has only been realized once, thereby no bar error are displayed. It is noticed that a highly pure α-TCP powder is obtained with only a 30 minutes dwell time. Nevertheless, in order to assure the total transformation of reactants into α-phase, when a higher amount of powder mixture is sintered, the following powders will be prepared with the advocated thermal treatment: 2 hours at 1250°C.

B) Preparation of the α-TCP control powder for the cement preparation

The appropriate thermal treatment has also been studied for the preparation of pure α-TCP (control powder). In any case, the heat treatment was based on the same model: an increasing ramp of 5°C/min followed by a 2-hours dwell, to cool down the samples inside the furnace afterwards.

The following graph shows the influence of the temperature, on the crystalline phase: repartition:

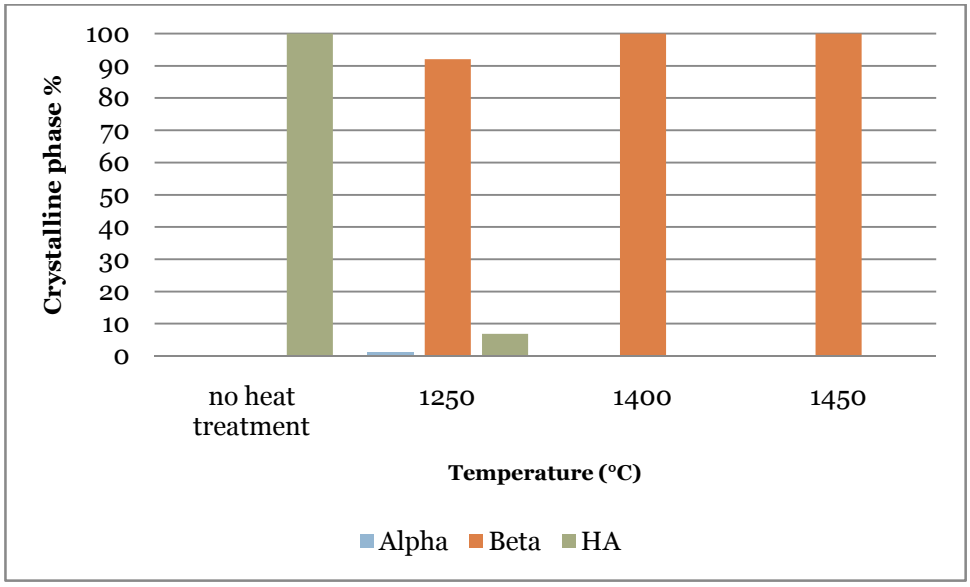

Fig 8.11: phase repartition of the control powder heated at several temperatures for 2 hours, cooling down the samples inside the furnace

Since the initial reactant is HA, without any thermal treatment, the phase obtained is, of course, HA. The heat treatment that had been chosen for the preparation of Si-α-TCP (a temperature of 1250°C for 2 hours) is not valid in the case of no adding silicon to the HA: it is composed for a 92% of β-TCP. Thus, the temperature was raised until 1400°C and 1450°C (limit of the oven) in order to reach a total decomposition of HA. At 1450°C the HA completely transforms, and β-TCP is the end-product because the samples are slowly cooled down. This can be understood by the phase diagram studied in the Calcium

Phosphates (chapter 4.2.5.), which indicates that the stable phase at room temperature is the β-TCP. Thereby, without silicon, α-TCP cannot be obtained if the samples are cooled down slowly.

From the phase diagram of the P_2O_5-CaO system (section 5.5.), it is known that a quenching is needed to stabilize the α-TCP phase at room temperature, being a metastable phase. Here is the influence of the quenching on the same heat treatments than seen reported previously:

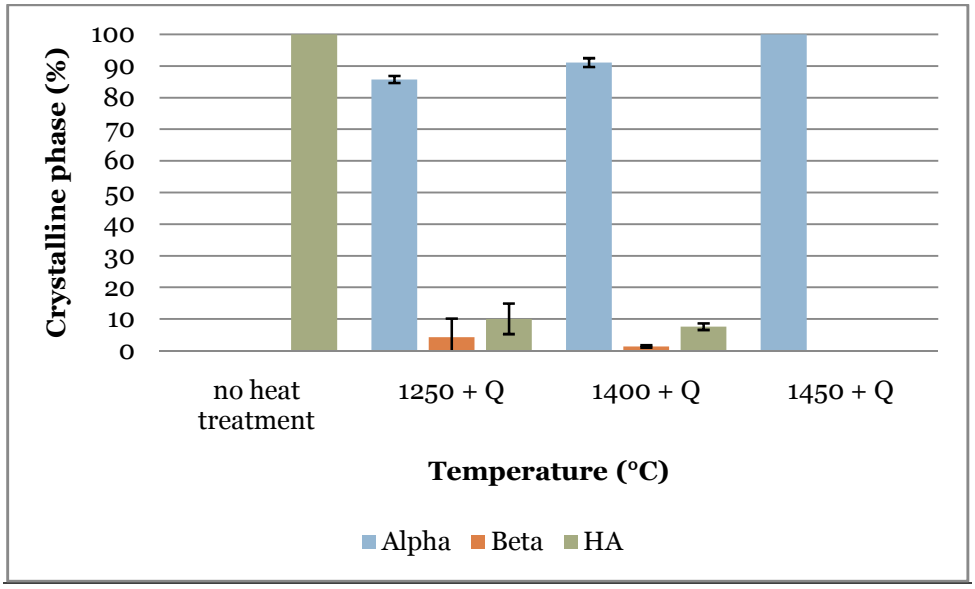

Fig 8.12: influence of the heat treatment on the phase composition of the control powder (the heat treatments have been followed by a Quench)

Although the quenching is essential for the formation of α-phase, heating the powder at 1250°C is not enough to obtain pure α-TCP. This is coherent with the results obtained when no quenching was applied, in both cases about a 10% of HA remains after the sintering. When increasing the temperature until 1450°C, the HA completely transforms into α-TCP, and this phase is maintained at room temperature due to the quench.

It is moreover observed, contrasting with the non-quenched samples, that a higher amount of HA is maintained when a quench is done. Indeed, when no quench is performed, a higher amount of HA transforms into β-TCP since the powder stays more time in the oven, and thus the transformation continues while the temperature is slowly decreasing.

The quench has not only an impact on the powder composition, but also on its specific surface area, as drawn in the following figure:

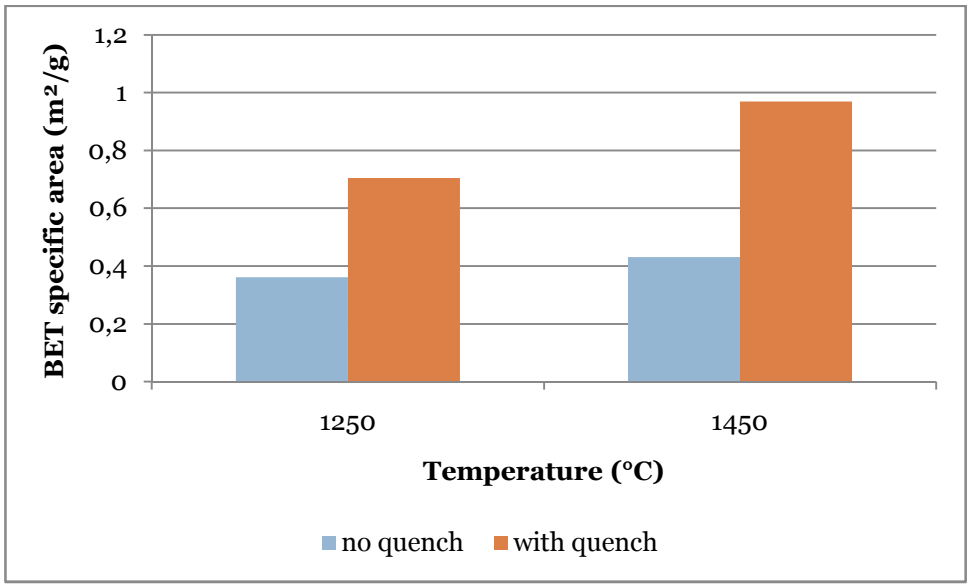

Fig. 8.13: Influence of the quench on the specific area of the control powder

The quench influences the particle size in a similar way that explained before. The longer the time the powder has been submitted at high temperature (when no quench is performed), the higher the particle size obtained, thereby decreasing its surface area. Consequently, the specific surface increases when a quench is performed.

Until here, it has been optimized the preparation of Si-α-TCP (by the appropriate proportion of silicon and the adequate heat treatment) and as well the conditions for the preparation of pure α-TCP (by the thermal treatment):

- The α-TCP doped with silicon is prepared with a SiO_2/HA molar ratio of 0.48, and heated up at 1250°C during 2h.

- The α-TCP free of silicon (control powders) is prepared using an HA without silicon addition, heat treated at 1450°C during 2 h and followed by a quench.

Having controlled the parameters for the obtaining of Si-α-TCP and α-TCP powders, the cements can be prepared.

8.3. Preparation and characterization of the Cements

8.3.1. Influence of grinding - particle size

As referred in the Materials and Methods section, grinding is an important step, previous to the preparation of the cements, in order to obtain the powder in an appropriate particle size, which significantly affects on the cements reactivity.

The following graph represents the effect of the grinding on the particle size for the Si-α-TCP powder and control powder:

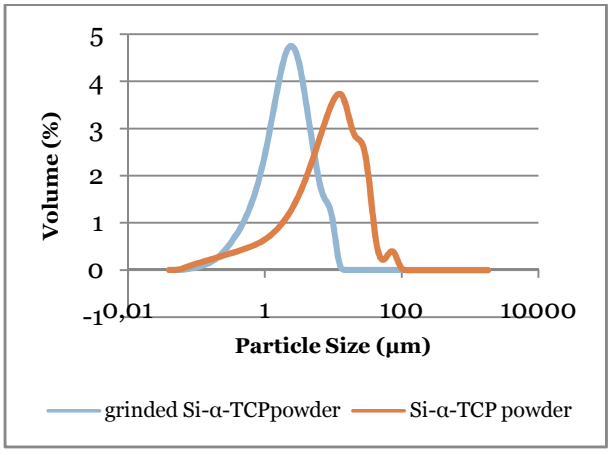

Fig 8.14: effect of the grinding on the particle size of Si-α-TCP

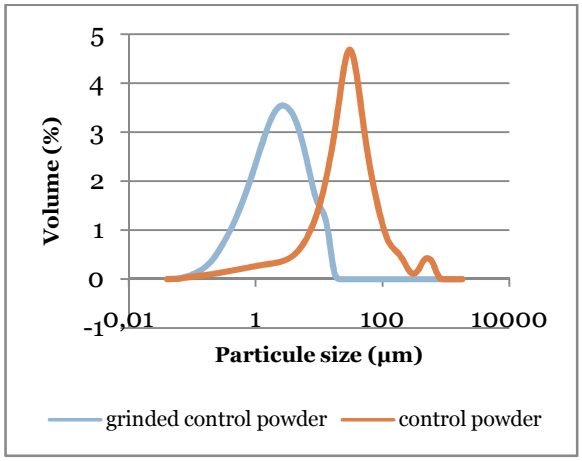

Fig 8.15: effect of the grinding on the particle size of the control powder

Thanks to the grinding, the mean particle size is reduced, which means that its surface area is increased, giving place to a more reactive material. The particle size distribution of the powder is more homogeneous, which will clearly lead to better cements, as the more uniform the raw material is, the more homogenous will be the crystals produced during the setting reaction.

The observation is the same in the case of the control powder: the particle size is more uniform and the mean particle size is smaller.

In the following graph are displayed both grinded powders:

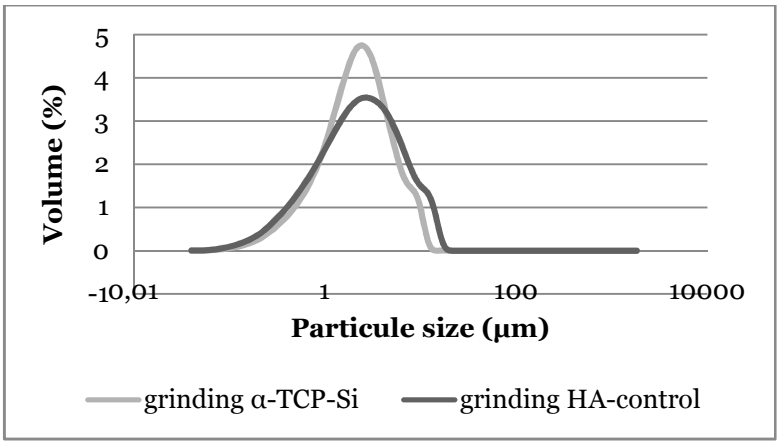

Fig 8.16: particle size distribution of the grind powder

The particle size distribution is similar for both powders: between 0.7 and 8 µm. One might remark from the table below that the mean particle size of the Si-α-TCP powder is not very different than that of the control powder. For this reason, it is expected that any difference that the cements reveal will be not due to the particle size differences, but to the silicon incorporation.

Mean particle size (µm)	Si-α-TCP	α-TCP (control)
Before grinding	13.12	52.87
After grinding	2.91	6.55

Table 8.4: mean particle size of the powders according to granulometry

The effect of the grinding was also characterized with the BET technique, as shown on the following figure:

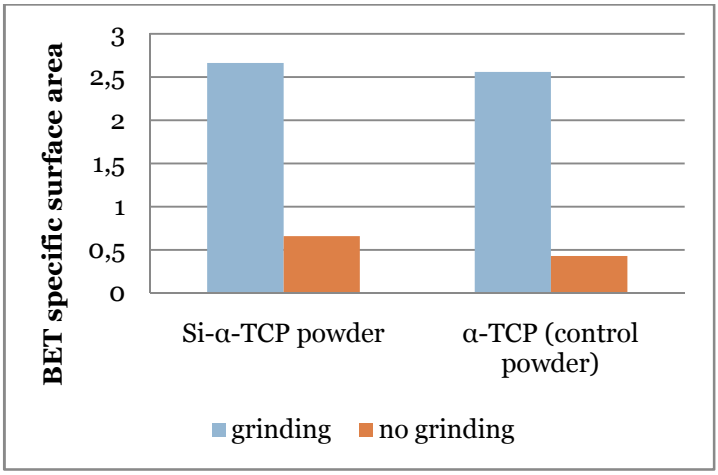

Fig 8.17: effect of the grinding on the specific surface area.

The effect of the grinding on the specific surface area is clear: since the mean particle size decreases, the specific surface increases, from 0.66 to 2.66m²/g for the Si-α-TCP and from 0.43 to 2.56m/g for the control powder.

The following SEM pictures show the grinded powders

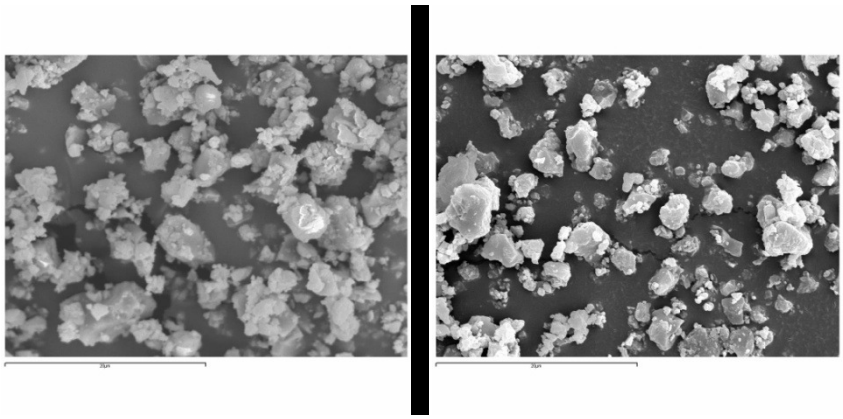

(a) (b)

Fig. 8.18: SEM pictures of the grinded powders (a): α-TCP (control powder) (b): Si-α-TCP powder

Again, it is verified that there is almost no difference between the two powders. Both particle sizes are between 0.5 and 10 μm. This is an important advantage in order to compare those cements which have been prepared from a Si-α-TCP, from those prepared using a silicon free α-TCP, allowing a better observation on the effect of the silicon.

8.3.2. REACTION KINETICS

As explained in detail in the "Materials and Methods" section, the cements prepared were stored in Ringer's solution at 37°C. Their mechanical and physic-chemical properties are tested at three different times: after 8 hours, 1 day, and 7 days spent in the Ringer's solution.

First, the crystalline phase proportion has been evaluated in order to know how fast the α-phase transforms into CDHA. Here is represented this evolution for both cements:

Using Si-α-TCP as reactant powder:

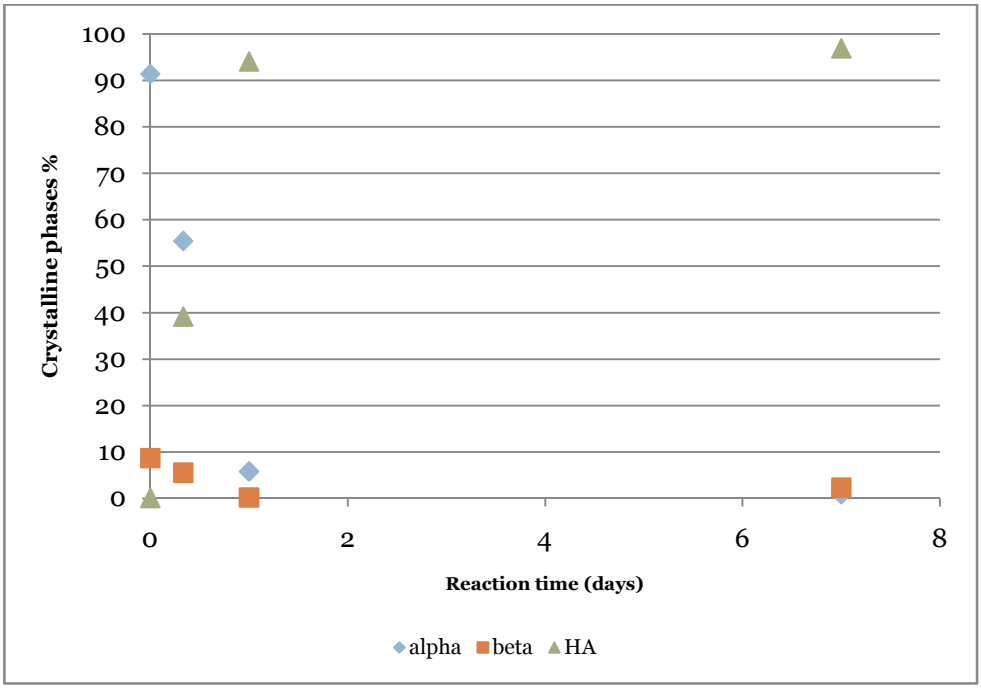

Fig. 8.19: percentage crystalline phases of the Si doped cements according to the time spent in Ringer's solution (0h, 8h, 1 day and 7 days)

Using α-TCP as reactant powder (control):

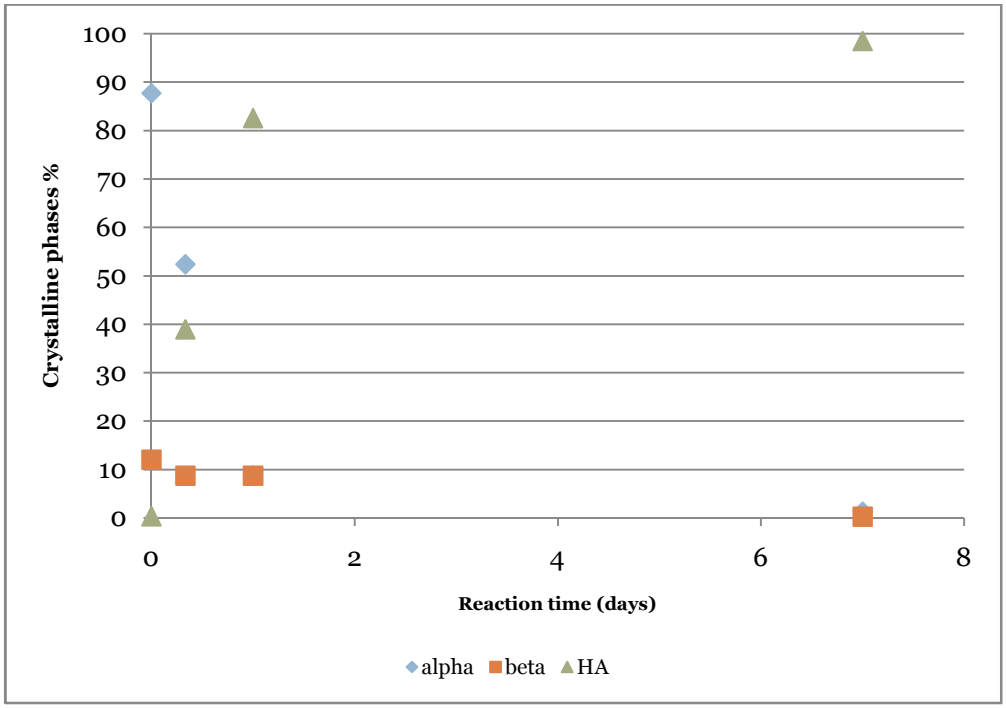

Fig. 8.20: percentage crystalline phases of the control cements according to the time spent in Ringer's solution (0h, 8h, 1 day and 7 days)

The graphics show that 8 hours spent in the Ringer's solution is not enough for the cement to transform completely into a CDHA, since the paste is still mainly composed for the α-phase. In contrast, after 1 day the reactant has transformed almost completely into CDHA phase. In both cases the reactivity of the setting reaction similar.

Since the cement has reached its final composition, a CDHA which is pretty stable, it is not necessary to test it further in the time.

The transformation of initial Si-α-TCP to HA compound was observed by FTIR technique. Here is the IR spectrum of the Si-α-TCP powder and the cements after various times spent in the Ringer's solution.

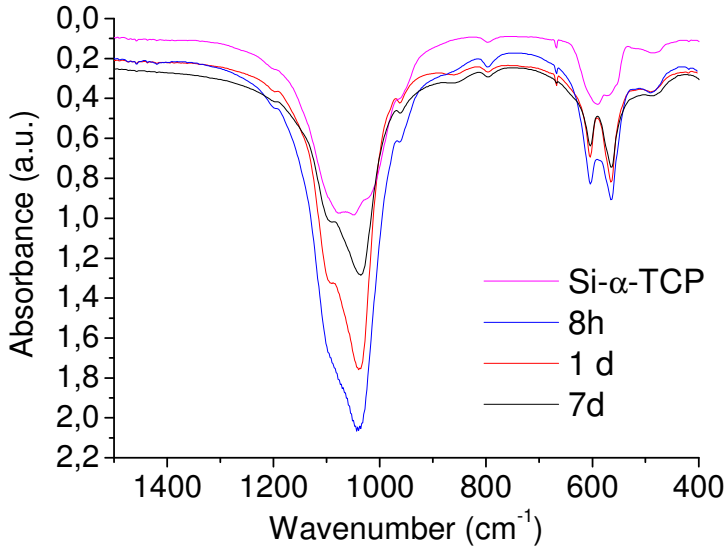

Fig. 8.21: Spectra of the Si-α-TCP powder and the Si-CDHA cements, after various time spent in the Ringer's solution.

In order to see the differences produced by the cement hardening reaction, we will just compare the initial reactant (Si-α-TCP) with the end-product, after a soaking in Ringer's of 7 days (Fig. 8.22).

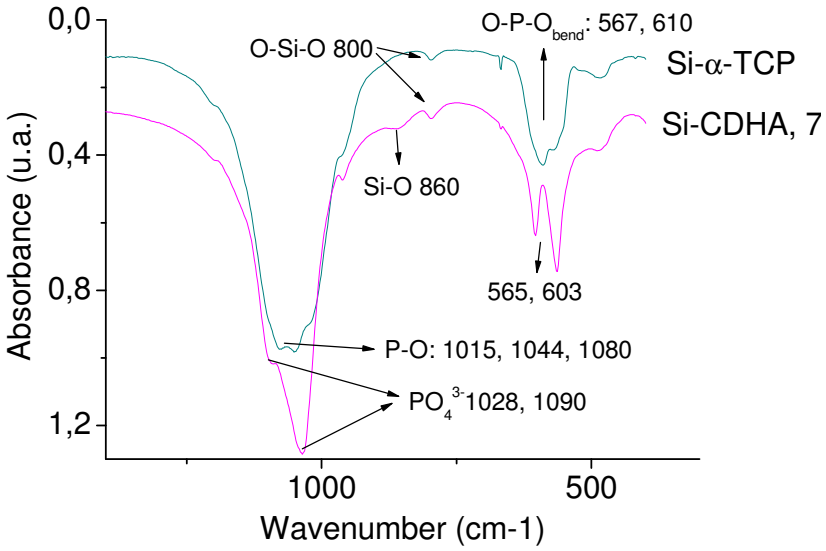

Fig. 8.22: IR spectra of the Si-α-TCP powder and Si-CDHA cement (after 7 days spent in Ringer's) with their corresponding bonds

Asymmetric P-O stretch band of Si-α-TCP, with weak bands at 1015, 1044 and 1080 cm^{-1} transforms to the band corresponding to vibration of PO_4^{3-} of CDHA, with corresponding bands at 1090 and 1028 cm^{-1}. Also, the O-P-O bending band of Si-α-TCP, which show weak bands at 567 and 610 cm^{-1}, evolve to differentiated peaks at 565 and 603 cm^{-1} when the CDHA is formed.

As for the Si-α-TCP powders, the peak corresponding to O-Si-O vibration is also observed with the cements at 800 cm^{-1}, which seem to indicate that SiO_2 has been introduced into the cements, although the SO itself shows this band at 814cm^{-1}.

Finally, no significant differences are observed in the IR spectra bands between both cement end-products (CDHA phase formed from initial reactants: α-TCP and Si-α-TCP), evaluated after 7 days in Ringer's solution, as it can be seen on the following spectra:

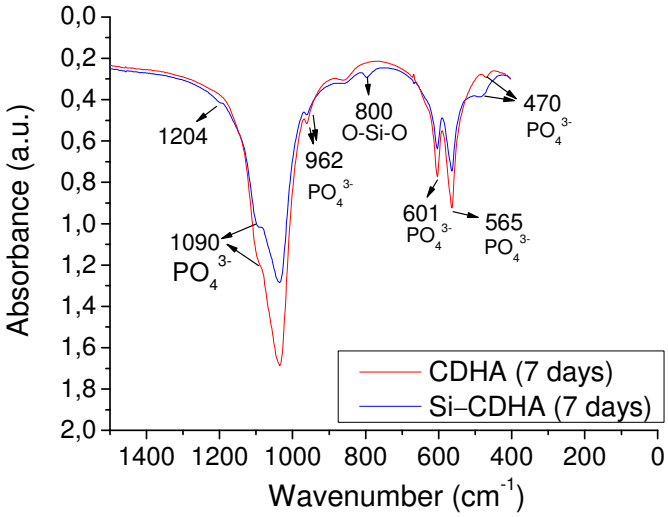

Fig.8.23 IR spectra of CDHA and Si-CDHA cement, after 7 days spent in Ringer's, with their corresponding bonds

The cements morphology has been observed with the SEM microscope. Here are some photos obtained of the control cements and the Si-doped ones, at different times spent in Ringer's.

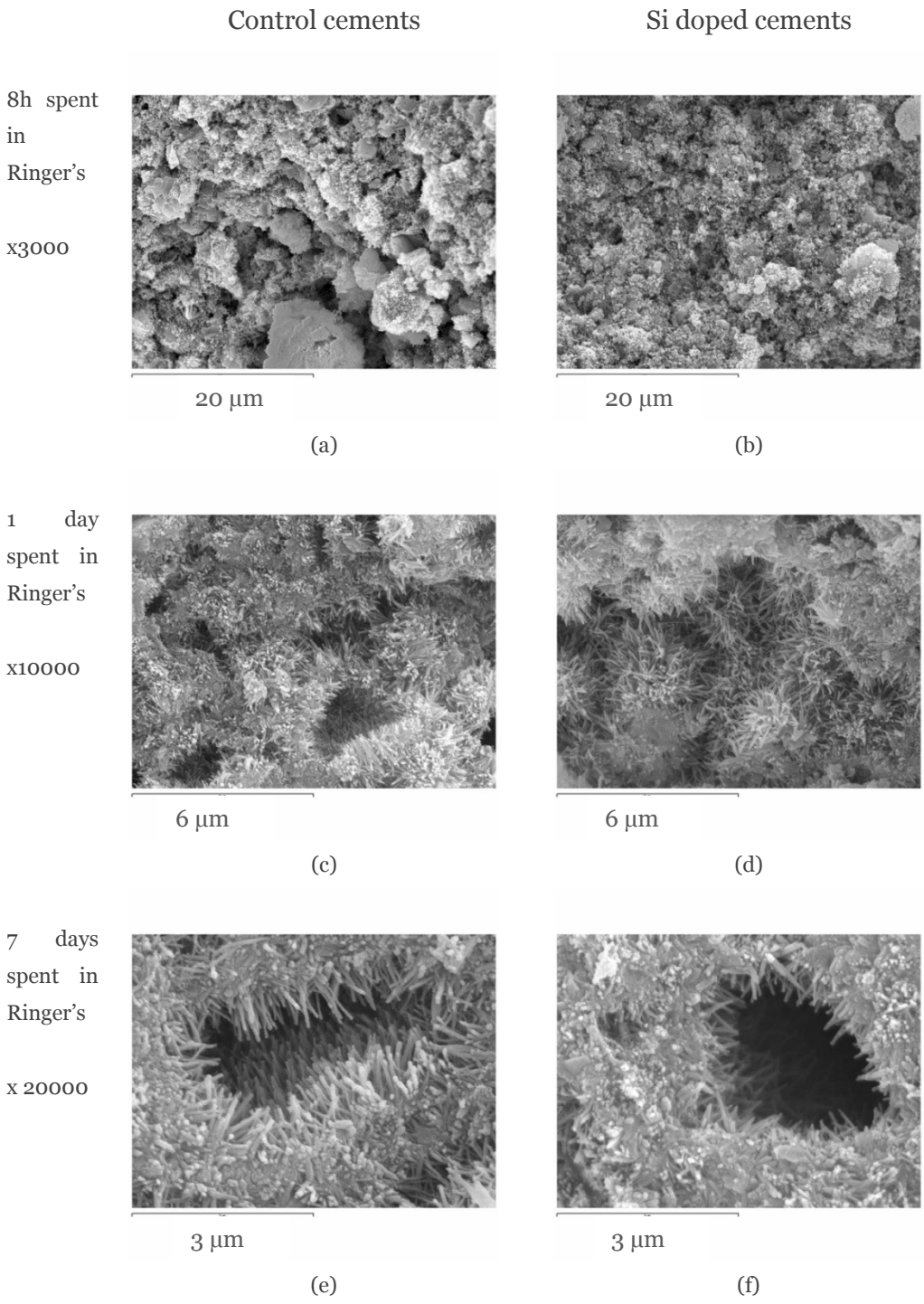

Fig. 8.24: SEM pictures of the cements: (a), (c), (e): control cements, (b), (d), (f): Si doped cements

Whatever time spent in Ringer's solution is considered; the morphology of both cements is the same. Nevertheless, it does change with time: as the transformation of α-TCP to CDHA occurs (between 8h spent in Ringer's and 1 day), from round particles (photos (a) and (b))

to needles like nanocrystals, (photos (c) and (d)).

On the figure below is represented the evolution of the cements specific surface area with the time spent in the Ringer's solution.

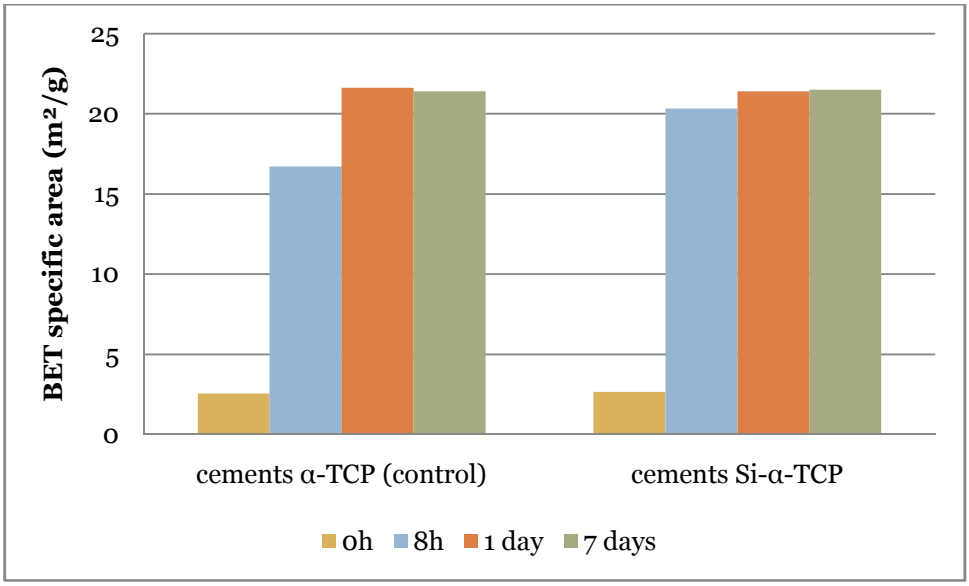

Fig. 8.25: Evolution of the specific surface area of the cements measured by N_2 absorption technique

Both cements follow the same tendency: the specific surface area increases with the time spent in Ringer's solution and seems to get stable afterwards. Moreover, it is noticed that the Si-α-TCP cements reach this equilibrium faster than the control cements.

Finally, is important to notice that the α-TCP powder (reactant for cements) has a much lower specific surface area that the CDHA formed during the cements reaction. This fact was shown as well by SEM pictures: the morphology of the cements changes from particles to needle like nanocrystals (Fig. 8.24.f).

Regarding the density, the cements have been characterized by two techniques: the helium pycnometry (skeletal density) and the mercury intrusion porosimetry (bulk density). Here are the results obtained for the skeletal density:

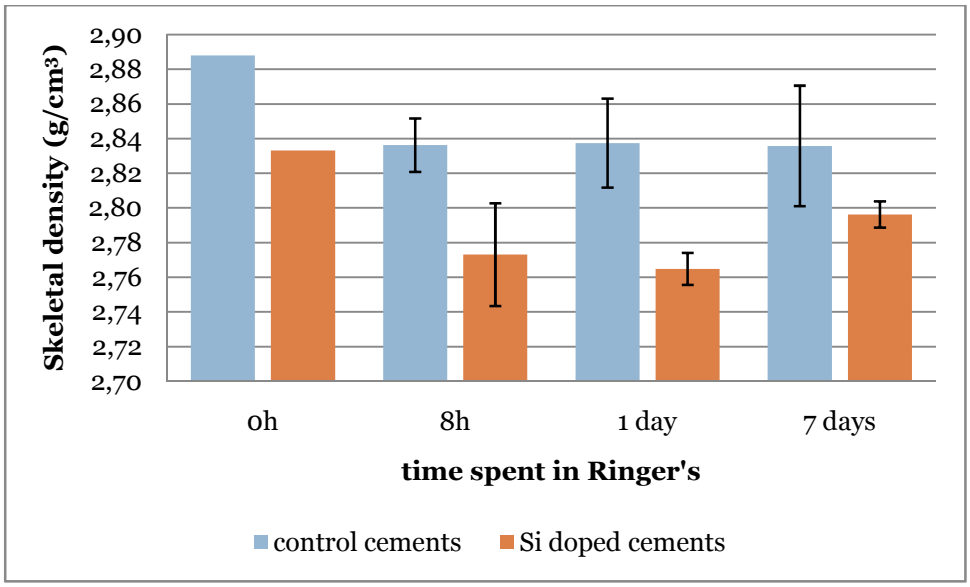

Fig. 8.26: Skeletal density of the cements, measured with the pycnometer (He)

The skeletal density of both cements types decrease after it has been stored in the Ringer's solution, when transforming from α-TCP to CDHA. However, after being immersed in Ringer's solution for 8 hours, the density does not change due to the CDHA stability.

Furthermore, it appears clearly that the skeletal density of Si-α-TCP and cements doped with silicon, are inferior to the analogue component when no silicon is added. Nevertheless, it is important to consider that we have an excess of SiO_2 which has not reacted and has a pretty lower skeletal density (2.20 g/cm³). This excess of SiO_2 decreases the mean value of skeletal density, being then difficult to compare the influence of silicon. If we suppose that anyway the reactants and end-products that contain silicon has a lower value than those that are silicon free, this could indicate:

- since the silicon (bulkier than phosphor) is introduced into the lattice, expanding the crystal lattice, hence the density decreases since the mass stays about the same;
- the defects produced into the cell due to the different charge between phosphorous and silicon ions, creates a predominant vacancies on oxygen ions in front of the excess on calcium ions.

Finally, the skeletal density found for CDHA is pretty close to those reported by Montufar et al. [70], who assumed a value of 2.71 g/cm³ for this component.

The following graphics show a complementary results found with MIP characterization

technique: the porosity and the bulk density of the cements. Both cements have been tested after 1 day and after 7 days in Ringer's solution.

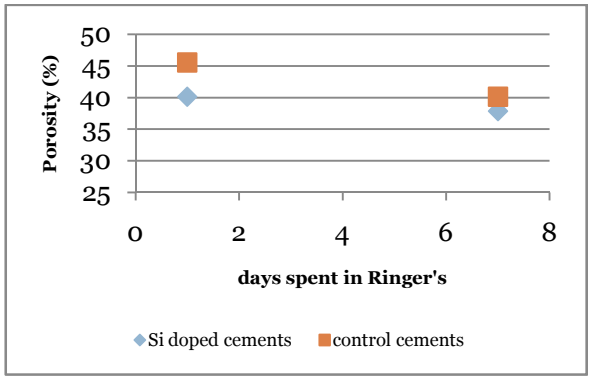

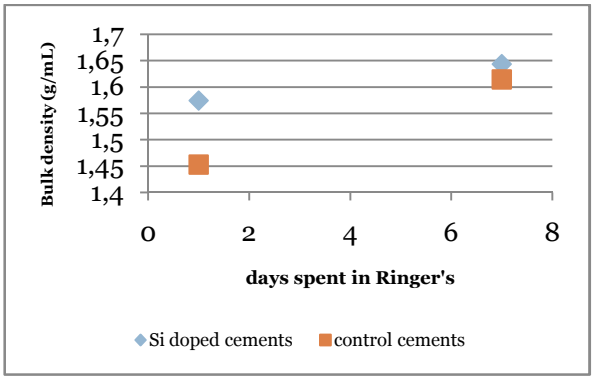

Fig 8.27 and 8.28 porosity and bulk density of the cements after 1 and 7 days in Ringer's as measuread by MIP

With time, it appears that the porosimetry decreases for both cements. On another hand, the bulk density increases. Indeed, since there is less pores on the material, it is denser.

Graphics of pores size distribution of cements, after having been in Ringer's solution for 1 day and 7 days are displayed below:

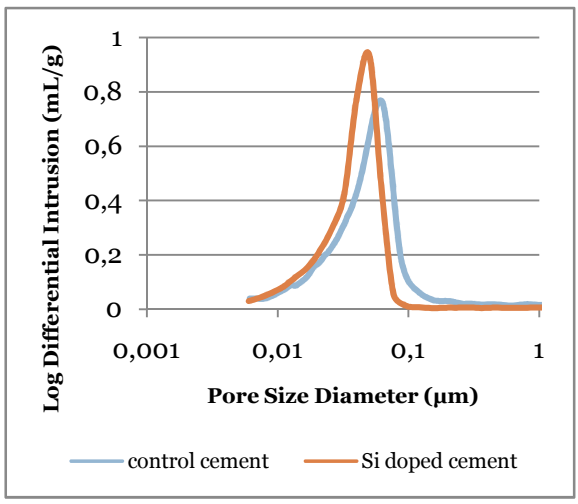

Fig. 8.29: pore size diameter of the cements measured by MIP after 1 day spent in Ringer's solution (both are between 0.03 and 0.08 µm)

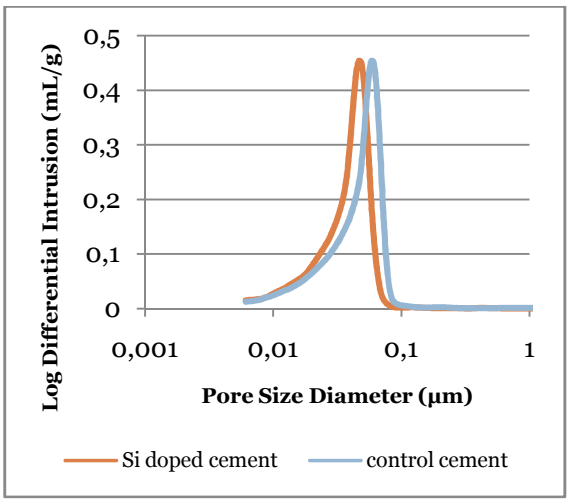

Fig. 8.30: pore size diameter after 7 days spent in Ringer's solution (for both cements between 0.4 and 0.7 µm)

Both cements, after being immersed in Ringer's solution for 1 day, show pore size diameters between the same values (from 0.03 to 0.08 µm). For those cements immersed

in Ringer's for 7 days, the pore size diameter distribution is also similar for both of them (between 0.4 and 0.7 μm).

The next graph shows the evolution of pore size distribution with time, for the cements doped with silicon:

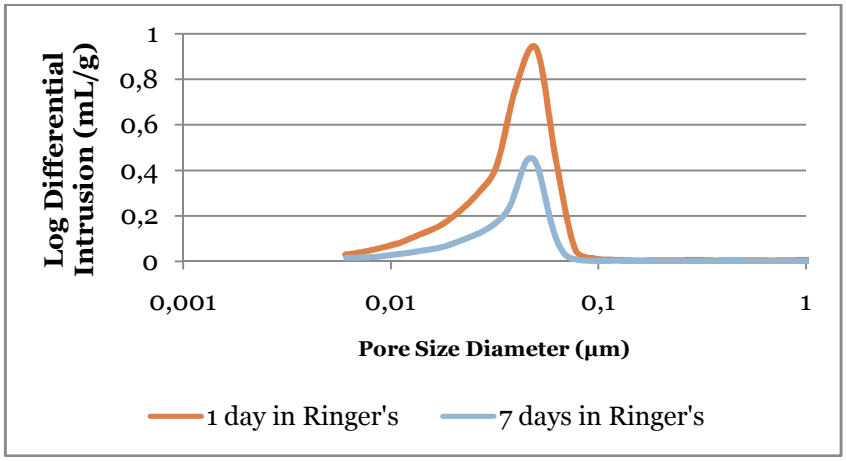

Fig 8.31: pore size diameter of the Si-doped cements according to the time they spent in the Ringer's solution

The amount of pores of the cement seems to be lower after having been immersed in Ringer's for 7 days than after 1 day. This is directly related with the decrease on porosity explained before, which comes from the same characterization technique. Nevertheless, the difference is not considered significant, as the composition is already stable after one day.

Another important property that must be evaluated in a material that has the potentiality to be incorporated into the body, are the mechanical properties. It has been evaluated the influence of the time spent in Ringer's solution on the maximum compression strength of cements. On the graph below are represented the resistance to compression of both cements types: with and without silicon.

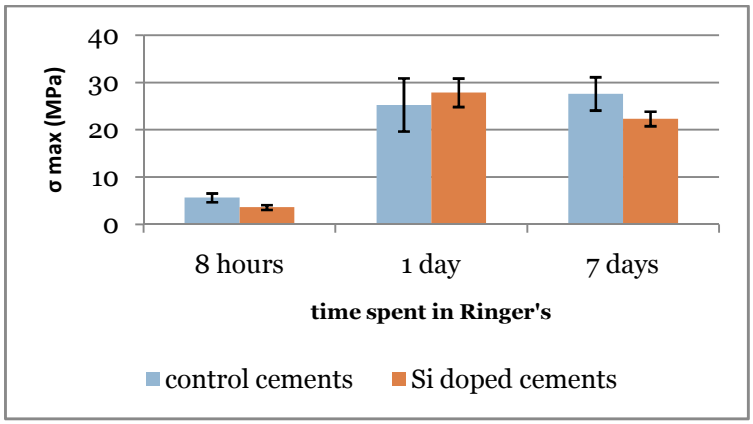

Fig 8.32: Resistance of the cements to compression, measured after various times spent in Ringer's

Using the information extracted of XRD technique, an increase on mechanical properties is expected during the CDHA formation, due to an increase of the entangled needle crystals. The similar morphologies revealed by SEM confirm this theory.

According to this figure, it seems that the resistance to compression increases with the amount of HA transformed. Thus, the strength that cements have after immersion in Ringer's solution for 1 day is higher than after 8 hours. After 1 day, as the transformation into CDHA is practically complete and this component is stable, the resistance to compression is maintained. Nevertheless, since the standard deviations of this figure are quite elevated, is difficult to make any strict affirmation about the changes on resistance of the cements

The values of cements resistance to compression obtained are higher than those corresponding to spongy bones (between 2 and 12 MPa). Nevertheless, this material should be applied in areas of low mechanical demand, as for example, as bone filler. Nevertheless, other studies show that these mechanical properties can be significantly increased by using an accelerant solution (2.5% of Na_2HPO_4) or adding HA seeds to the powder [71].

Although it can be appreciated the incorporation of silicon into the end product of cements, there have not been revealed important differences on the physic-chemical properties of these cements (reactivity of the reaction, morphology, specific surface area, porosity and mechanical properties). This fact would be useful, for example, in future *in vitro* studies, in which cells would be put in contact with the surface of the material. As was revealed that the morphology of cements is similar at different times, the differences that can be appreciated in this *in vitro* study would be only due to the silicon incorporation.

9. CONCLUSIONS

The two goals proposed for this project have been successfully achieved: not only the α-TCP stabilized with silicon have been prepared but also the efficiency of the resulting Si-α-TCP as calcium phosphate cements reactant has been proved.

One of the main advantages of obtaining Si-α-TCP is the less-energetic and drastic demand of the heat treatment: the silicon incorporation allows obtaining the α-TCP phase at lower temperature and without quenching.

The Si-α-TCP has been prepared by using a new method, which is also very simple: the wet milling of the reactants, followed by a subsequent thermal treatment. Thereby, the reactants ratio, the milling conditions and the heat treatment have been optimized, and the following parameters have been selected:

- SiO_2/HA molar ratio of 0.48
- Wet milling at speed of 350 rpm for 30 min (for 20g of HA and 50 mL of water)
- Thermal treatment of 1250ºC for 2h without quenching

Cements have been prepared by mixing Si-α-TCP powder with water as liquid phase, in a liquid to powder ratio of 0.32. These cements have been characterized after different reaction times, but further studies will be needed in order to evaluate the silicon incorporation into the CDHA lattice.

It has been demonstrated in this project that Si-α-TCP can be used as a reactant in the preparation of calcium phosphate cements, with the same setting parameters than CDHA cements.

The benefit of the incorporation of silicon in calcium phosphate cements theoretically leads to a higher bioactivity and also enhances the cell differentiation and proliferation. Nevertheless, these experiments are still to be performed. Since both cements (Si-CPCs and CPCs) have similar physic-chemical properties, it will be possible to evaluate the influence of silicon.

10. RECOMMENDATIONS AND FUTURE PERSPECTIVES

10.1 RECOMMENDATIONS

The experience acquired during the realization of this project brings out two main points which could be enhanced:

- Experimental conditions of the Si-α-TCP preparation:

Since it was observed that a dwell time of 30 min was enough to quantitavely obtain α-phase, it should be checked if this thermal treatment is also efficient enough when a higher quantity of material is prepared. It could also be studied if a lower thermal treatment would lead to the same product.

- Physic-chemical and mechanical properties of cements:

Deeper analysis of IR spectra should be done in order to evaluate the incorporation of silicon into the CDHA lattice. This incorporation could also be verified by using a high resolution TEM. This technique is very accurate and the cell parameters obtained by the crystal pattern analysis is very precise.

Moreover, the mechanical properties of the cements could be optimized. That could be done using accelerant solution to the liquid phase or adding seeds during the preparation.

10.2 FUTURE PERSPECTIVES

As future perspectives, the following points should be studied in order to use these cements in orthopedic applications:

- An exhaustive characterization of the silicon incorporation in the lattice, for both α-TCP and CDHA, using IR, XRD and high resolution TEM.
- The enhancement of the biologic properties should be verified. An *in vitro* study at long time could be performed in order to see if silicon added in cements enhances the cells proliferation and differentiation.
- The improvement of the apatite layer formation due to the silicon incorporation on the surface should also be checked. A simple experiment would consist in

introducing set cements in SBF (Simulated Body Fluid), which stimulates the apatite cape formation.

- Finally, further study on the β-α transition will be carried out, evaluating the phase transformation *in situ* (from room temperature to 1500°C). This study will give important information on how the transformations are produced, and will help to adjust the best thermal treatment. This project proposal has already been accepted by the Institute Laue-Langevin in Grenoble, France, and will be performed by using neutrons diffraction.

11. ECONOMIC ASPECTS AND ENVIRONMENT IMPACT

In this section is estimated the cost of the whole project, in terms of economy and also regarding to the environment impact.

11.1 ECONOMIC ASPECTS

The economic aspects have also been divided in two sections, one focusing to the materials used, and the other one estimating the cost related to the characterization techniques. . These costs do not include the energetic cost neither the wear and tear cost of the machines.

11.1.1. MATERIAL

Firstly are quantified the raw materials used during the Project, including all necessary reactants for the Si-α-TCP fabrication, and the subsequent cement preparation.

The following tables present the approximately costs for the reactants used:

Product	Quantity	Cost (€)
Hydroxiapatite CalbioChem	320 g	464
SO	30g	38
NaCl (Ringer's solution preparation)	9g	0.8
	TOTAL COST	**502.8 €**

Table 11.1. Estimated cost for raw materials

11.1.2. CHARACTERIZATION TECHNIQUES

Characterization technique	Try or hour cost (€)	Total cost (€)
XRD	6.74	230
Compression resistance	3.02	21.14
Porosimetry	63	250
Pycnometry	0.50	10

SEM	31.5	157.5
TEM	42	210
IR	-	0
Granulometry	41.8	83.6
ICP OES	41.83	376.47
ICP MS	44.04	264.24
Scanner negatives	13.06	26
N_2 absorption (BET)	7.32	250
	Total cost of the characterization techniques	**1878.95**

Table 11.1.2: Estimated cost for characterization techniques

11.2. ENVIRONMENT IMPACT

The project has been carried out with an overall regard towards the environment: the raw material used was calcium phosphate, the main inorganic component of hard tissues. The CaP does is not harmful concerning the environment, due its natural character.

Moreover, in order to diminish at maximum any possible contamination, the Biomaterials group of the ETSEIB has a strict waste policy: all the cements wasted were stored in specific garbage so that they are treated apart from the regular wastes. They are also selectively stored gloves and other plastic residues, acid, bases, oily liquids, and others.

About the characterization techniques used, the mercury porosimetry is the one that can cause a higher impact for the environment. This is because mercury is a dangerous substance, since it is a heavy and non biodegradable metal. Therefore, it has a high bioaccumulation potential into the living organisms, being toxic for all the living species [72]. In order to minimize the dangerous effect of mercury, the characterizations that use this substance have been realized under conditions which avoid the evaporation of the metal, and using a extractor fan in the room. Special recipients to contain the mercury are used while washing the pycnometer and the residues are stored and delivered to the specific unit of waste treating. However, porosimetry has not been used a lot in this project (4 experiments) so the impact on the environment is pretty low.

ACKNOWLEDGEMENTS

First of all, I would like to thank Maria Pau Ginebra for the opportunity she gave me to work in this project, and who made me discover a whole new field of the materials engineering. I would also like to thank her for the time and consideration she had for me, and in a more general manner the help she gave to the project. The realization of this master's thesis could have been done without her dynamism and implication.

I would also like to address my special thanks to Gemma Mestres for everything she has done in this project. Gemma, gràcies per la teva paciència, per la teva motivació, el teu entusiasme i el teu buen humor!
Moltes graciès per l'ajuda proporcionada al llarg de tot el projecte sense la qual no hauria estat possible la seva realització... i per ensenyarme una mica de català!

Then, I would like to show my gratitude to Meritxell Molmeneu for the help and time she put into my project, and also for creating nice working conditions in the biomaterial department.

My appreciation also goes to Roman, Montse and Edgar who always had the time and patience to answer to my questions about the calcium phosphate cements.

Finally, I would like to thank all the persons working in the biomaterials department, especially the proyectistas for having shared this adventure with me. Without their availability and good moods, the realization of this project would never have been so pleasant.

BIBLIOGRAPHY

[1] United Nation Expert Group Meeting on Social and Economic Implication of Changing Population Age Structure A global Overview on social security in the age of longevity, Roland Sigg, International Security Association, Geneva. (2005)

[2] Arnold C. The skeletal system. Lerner Publishing Group (2004)

[3] Arnold,C. The skeletal system. Lerner Publishing Group (2004).

[4] Kokubo T, Kim HM, Kawashita M. Novel bioactive materials with different mechanical properties. Biomaterials 24 (2003) pp 2161-2175

[5] Frank H, Netter MD. The Netter Collection of Medical Illustrations – Muskuloskeletal System. Part I: Anatomy, Physiology and Metabolic Disorders p 170

[6]National Yang Ming University (Taiwan) (2008)
http://dlsm.ym.edu.tw/lesson/five.files/81.GIF

[7] http://www.c14dating.com/bone.html#apatite

8 Bronner F. Metals in Bone: aluminum, boron, cadmium, chromium, lead, silicon, and strontium, Principles of bone biology (1996)

[9] http://www.ncbi.nlm.nih.gov/books/bv.fcgi?rid=mcb.section.6542

[10] Bronner F, Farach-Carson MC, Rubin J. Bone resorption, Springer (2005)

[11] Ben-Nissan B. Nanoceramics in Biomedical Applications, Materials Research Society, Col 29 N°1 (January 2004)

[12] Czenuszka J. Biomaterials under the microscope, Material World, vol. 4 (1996), pp 452-53

[13] Strnad J, Strnad Z and Esták J, Physico-chemical properties and healing capacity of potentially bioactive titanium surface, 2007, Journal of Thermal Analysis and Calorimetry, Vol. 88

[14] Heness G, Ben-Nissan B. Innovative Bioceramics in Materials Forum, Vol. 27 (2004)

[15] Stol M, Smetana K. Jr, Korbelar P, Adam M. Poly(Hema)-Collagen Composite as a Biomaterial for Hard Tissue Replacement, Biomedical Polymers Conference, Jerusalem , (1993), vol. 13, nº 1-4 (25 ref.), pp. 19-20

[16] Vagoa R, Plotquinb D, Buninb A, Sinelnikovc I, Atarb D and Itzhakd D. Hard tissue remodeling using biofabricated coralline biomaterials, Journal of Biochemical and Biophysical Methods, Vol 50, Issues 2-3, 4 (January 2002) pp 253-259

[17] Albee, F.H. Studies in bone growth: triple calcium phosphate as a stimulus to osteogenesis. Annals of Surgery 71 (1920) pp 32-41

[18] Getter L, Bhaskar S, Cutright D, Perez B, Brady J, Driskell T, O'Hara M. Three biodegradable calcium phosphate slurry implants in bone. Joural of Oral Surgery. 30 (1972) pp 263-268

[19] Köster K, Karbe E, Kramer H, Heide H, König R. Experimenteller Knochenersatz durch resorbierbare Calciumphosphat-Kermaik. Langenbecks Arch. Chir.341 (1976) pp 77-86

[20] Dorozhkin, S.V. Calcium orthophosphate cements for biomedical application. Journal of Materials Sceice 43 (2008) pp 3028-3057

[21] Driessens F, Verbeeck R. Relation between phyico-chemical solubility and biodegrability of calcium phosphates. In: de Putter C, de Lange GL, de Groot K, Lee AJC. Eds Implant materials in biofunction. Advances in Biomaterials. Amsterdam: Elsevier (1988) pp 105-111

[22] Bohner M. Calcium orthophosphates in medicine: from ceramics to calcium phosphate cements.

[23] Barnes, Mary W.; Klimkiewicz, Maria; Brown, Paul W. Hydration in the system Ca_2SiO4-$Ca_3(PO_4)_2$ at 90ºC. Phase Equilibria. Journal of the American Ceramic Society 75 (1992) pp 1423-1429.

[24] Ginebra MP, Fernandes E, De maeyer EAP, Verbeeck RMH, Boltong MG, Ginebra J, Driessens FCM, Planell JA. Setting Reaction and Hardening of an Apatitic Calcium Phosphate Cement

[25] Brown W, Chow L. Dental restorative cement pastes. US Patent No. 4518430, 1985

[26] Kamerer DB,Hirsch BE, Snyderman CH, Costantino P, Friedman CD. Hydroxyapatite cement: a new method for achieving watertight closure in transtemporal surgery. Am J Otol 15 (1994) pp 47-49

[27] Constantz BR, Ison IC, Fulmer MT>, Poser RD, Smith ST, VanWagoner M, Ross J, Goldstein SA, Jupiter JB, Rosenthal DI. Skeletal repair by in situ formation of the mineral phase of bone. Science 267 (1995) pp 1796-9

[28] E. Fernandez, F.J Gil, M.P. Ginebra, F.C.M. Driessens, J.A. Planell, Calcium phosphate bone cement for clinical applications, Part I: solution chemistry, Journal of Materials Science,(1999) pp 169-176

[29] Vereecke G, Lemaître J. Calculation of the solubility diagrams in the system $Ca(OH)_2$-H_3PO_4-KOH-HNO_3-CO_2-H_2O. J. Crystal Growth 104 (1990) pp 820-832

[30] Ginebra M.P., Driessens F.C.M., Planell J.A. Effect of the particle size on the micro and nanostructural features of a calcium phosphate cement: a kinetic analysis. Biomaterials 25 (2004) pp 3453–3462

[31] Ginebra MP, Calcium phosphate bone cements (chapter 10)

[32] Driessens FCM, Boltong MG, Bermudez O, PLanell JA, Ginebra MP, Fernandez E. Effective formulations for the preparation of calcium phosphate bone cements. J Mater Sci Mater Med 5 (1994) pp 167-70

[33] E. M. CARLISLE, Ciba. Found. Symp. 121 (1986) p 123

[34] E. M. CARLISLE, Sci. Total Environ. 73 (1988) p 95

[35] Alexandra E. Porter, Nelesh Patel, Jeremy N. Skeeper, Serena M. Best, Willium Bonfield. Effect of sintered silicate-substituatd hydroxyapatite on remodeling processes at the bone implant interface

[36] Fix, W.; Heymann, H.; Heinke, R. Journal of the American Ceramic Society 52 (1969) pp 346–7.

[37] M. Sayer, A.D. Stratilatov, J. Reid, L. Calderin, M.J. Scott, X. Yin, M. MacKenzie, T.J.N. Smith, J.A. Hendry, S.D. Langstaff. “Structure and composition of Silicon-stabilized tricalcium phosphate”, Biomaterials 24 5(2003) pp 369-382

[38] R.L. Reis, S.Weiner. Learning from nature how to design new implantable biomaterials is. Springer Netherlands (2004)

[39] Landi E, Tampieri A, Mattioli-Belmonte M, Celotti G, Sandri M, Gigante A, Fava P, Biagini G. Biometric Mg and Mg,CO3 substituted hydroxyapatites: synthesis, characterization and in vitro behavior. Journal of the European Ceramic Society 26 (2006) pp 2593-2601

[40] Hall DA, Stevens R. Effect of water content on the structure and mechanical properties of magnesia-phosphate cement mortar. Journal of the American Ceramic Society 81 (1995) pp 1550-1556

[41] Mastrogiacoma M, Muraglia A, Komlev V, Peryin F, Rustichelli F, Crovace A, et al. Tissue engineering of bone: search for a better scaffold. Orthod Craniofacial Res 8 (2005) pp 277–84.

[42] Pietak A. The role of silicon in Si-TCP bioceramics: a material and biological characterization. Kingston, Ont., Canada: Queen's University; (2004).

[43] Hing K, Revell P, Smith N, Buckland T. Effect of silicon level on rate, quality and progression of bone healing within silicate substituted porous hydroxyapatite scaffolds. Biomaterials 27 (2006) pp 5014–26.

[44] Mastrogiacoma M, Corsi A, Francioso E, Di Comite M, Monetti F, Scaglione S, et al. Reconstruction of extensive long bone defects in sheep using resorbable biocermics based on silicon stabilized tracalcium phosphate. Tissue Eng 12 (2006) pp 1261–73.

[45] Botelho C, Brooks R, Best S, Lopes M, Santos J, Rushton N, et al. Human osteoblast response to silicon-substituted hydroxyapatite. J Biomed Mater Res A 79 (2006)pp 723–30.

[46] Patel N, Best S, Bonfield W, Gibson I, Hing K, Damien E, et al. A comparitive study on the in vivo behavior of hydroxyapatite and silicon substituted hydroxyapatite granules. J Mater Sci Mater Med 13 (2002)pp 1199–206.

[47] Reid, Joel W.; Fargo, Karen; Hendry, Jason A.; Sayer, Michael. The influence of trace Mg content on the phase composition of Si-stabilized CaP powders. Materials Letters 61 (2007) pp 3851-3854

[49] Reid, J.W.; Tuck, L.; Sayer, M.; Fargo, K.; Hendry, J.A. Synthesis and characterization of single-phase silicon-substituted α-tricalcium phosphate. Biomaterials 27 (2006) pp 2916–2925.

[50] El Briak-Ben Abdeslam H, Ginebra MP, Vert M, Boudevill P. Wet or dry mechanochemical synthesis of calcium phosphates? Influence of the water content on DCPD-CaO reaction kinetics. Elsevier (2008) pp 378-386

[51] De Wolff, P. Technisch Physische Dienst, Delf, The Netherlands. PDF Card #09-0348

[52] De Wolff, P. Technisch Physische Dienst, Delf, The Netherlands (1957). PDF Card #09-0169

[53] Wolff, P. Technisch Physische Dienst, Delf, The Netherlands. PDF Card #09-0432.

[54] Mathew, M.; Schroeder, L.W.; Dickens,B.; Brown, W.E. The crystal structure of alpha-$Ca_3(PO_4)_2$. Acta Crystallographica B (24,1968-38,1982) 33.(1977) 1325-1333

[55] Dickens, B.; Schroeder, L.W.; Brown, W.E. Crystallographic studies of the role of Mg as a stabilizing impurity in beta-$Ca_3(PO_4)_2$. The crystal structure of pure beta-$Ca_3(PO_4)_2$. Journal of Solid State Chemistry 10 (1974) 232-248.

[56] de Andrade, A.V.C.; da Silva, J.C.Z.; Paiva-Santos, C.O.; Weber, C.; dos Santos Utuni, V.H.; Tebcherani, S.M.; Ferreira Borges, C.P.; da Costa, E.; Martinez Manent, S. Synthesis and crystal phase evaluation of hydroxylapatite using the Rietveld - maximum entropy method. Ceramic Engineering and Science Proceedings 25 (2004) 639-645.

[57] Rodriguez-Carvajal J. Fullprof.2k (Version Feb2007 – LLB JRC) (CEA-CNRS)

[58] Ginebra MP, Driessens FCM, Planell JA Effect of particle size on the micro and nanostructural feature of a calcium phosphate cement: a kinetic analysis. Biomaterials 25 (2004) pp 3453-3462

[59] Brunner TJ, Grass RN, Bohner M, Stark WJ. Effect of particle size, crystal phase and crystallinity on the reactivity of tricalcium phosphate cements for bone reconstruction. Journal of Materials Chemistry 17 (2007) pp 4072-4078

[60] Brunauer S, Emmett PH, Teller E. Adsorption of Gases in Multimolecular Layers. Journal of the American Chemestry Society 60 (1938) pp 309-319

[6161] Stanley BH, Thornton T. What is "BET Surface Area" and How Does it Affect the Performance of a Battery? Micromiritics Instrument Corporation

[62] Webb PA, Volume and Density Determination for Particle Technologists. Micromeritics Instrument Corporation (2001)

[63] Ando J: Bulletin of the Chemical Society of Japan Vol. 31 No. 2 (1958) pp 196-201

[64] Cusco R, Guilian F, de Aza S, Artus L. Jouranl of European ceramic society 18 (1998) pp 1301-1305

[65] Xu JL, Khor KA,. Chemical analysis of silica doped hydroxiapatite biomaterials consolidated by a spark plasma sintering method, Journal of inorganic Biochemestry vol 101, issue 2, (Feb 2007) pp 187-195

[66] Blakesee KC, Condrate SR RA. Journal of the American ceramic society 54 (1971), pp 559-563

[67] Calleja W, Falcony C, Torres A, Aceves M, Osoro R. Thin Solid Films (1995) p 270

[68] Sayer, M.; Stratilatov, A.D.; Reid, J.; Calderin, L.; Stott, M.J.; Yin, X.; MacKenzie, M.; Smith, T.J.N.; Hendry, J.A.; Langstaff, S.D. Structure and composition of silicon-stabilized tricalcium phosphate 24 (2003) pp 369-382.

[69] Hollenstein Ch, Howling AA, Courteille C, Magni D, Scholtz Odermatt S, Kroesen GMW, Simons N, de Zeeuw W, Scharzenbach W. Silicon Oxide Particle formation in RF plasmas investigated by infrared avsorption spectroscopy and mass spectroscopy. Journal of Physics D: Applied Physics (August 1997)

[70] Montufar EB, Gil C, Traykova T, Ginebra MP, Planell J. Foamed beta-Tricalcium Phosphate Scaffolds, Key Engineering Materials Vols. 361-363 (2008) pp 323-326

[71] Ginebra Molins MP, Desarrollo y caracterización de un cemento óseo basado en fosfato tricálcico-α para aplicaciones quirúrgicas. PhD thesis presented at the Universitat Politècnica de Catalunya.

[72] Graeme, K.A, Pollack, C. V Jr. Heavy metal toxicity, Part I: arsenic and mercury.J Emerg Med.Jan-Feb 1998;16: pp 45-56.